A Comparison of airborne and ground Electromagnetic data near the Grand Canyon

L.J. Davis and R.W. Groom,
Petros Eikon Inc.

February 2010

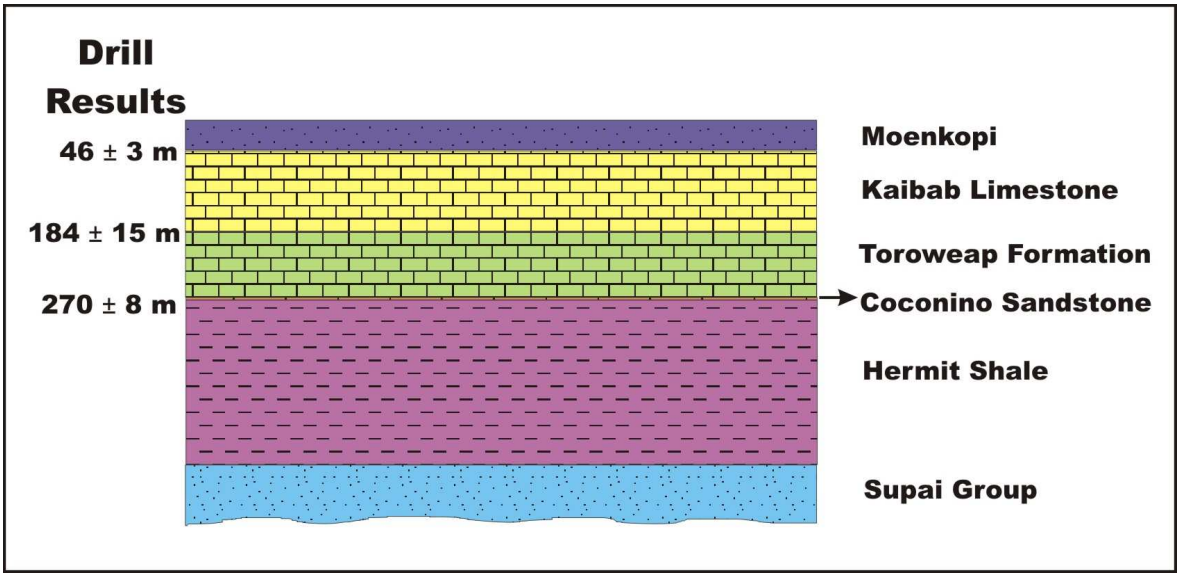

Executive Summary

Airborne time-domain electromagnetics (TEM) is used extensively in mineral exploration for locating conductors. In this study, we examine to what extent airborne TEM may also be used for quantitative geological interpretation, the resolution capabilities of various airborne TEM systems and the comparison of the resolved structures to ground EM data.

Three airborne surveys (MEGATEM, GEOTEM, and VTEM) were flown for Uranium One over a calibration site near the Grand Canyon as a contractual condition to much larger surveys. Ground TEM data (PROTEM) was later collected along with other ground EM data. The geology at the site is a thick, flat-lying sedimentary sequence. Our objective was to determine the ability of the ground data to resolve the sedimentary sequences and whether the airborne data would calibrate with the ground TEM. We wished to understand thoroughly the differences in resolution between the different systems and reasons, if any, for different structural interpretations from the different systems.

An excellent model was developed to fit the ground TEM data with corroboration of the other ground EM data. The model was in agreement with drilling data, other information at the site and general geological knowledge. The wide-offset configuration of the ground TEM data was critical for resolving the deeper geology.

The ground TEM model for the resistivity depth sequence which was confirmed by drill results and other ground EM data, was then used to evaluate the MEGATEM and GEOTEM. Using the waveform files supplied by Fugro Airborne head office, the pulse width, dipole moment and window positions were carefully determined. Modeling of the freespace response also enabled us to check the geometry of the system such as instrument offset and tilt as well as to study the

bandwidth of the system. When using low upper frequency bandwidths of 4 kHz and 6 kHz for the MEGATEM and GEOTEM respectively, the ground model fit the airborne data over the ground loop centered at 5200N. Farther south, from 4200N south to 3000N, these two airborne EM surveys show a slight but definite increase in shallow conductance though this is not observed in the PROTEM data. The most likely possibility is a layer of lower resistivity within the Moenkopi or at its base to which the PROTEM survey is not particularly sensitive at these offsets. The other ground EM data was not of sufficient quality to determine if such a small increase in conductance existed.

VTEM waveform files were provided by the survey crew for the flight. The waveform file is a time derivative series and thus is likely the system response at high altitude. This is not known precisely although the questions have been asked of Geotech personnel.

Careful study with the waveform files led us to conclude that the nature of the pulse was different from what U1 had requested. Precise modeling studies determined that while the nature of the system turn-on has a small effect on the response, the turn-off, particularly the rate of turn-off at the very end of the pulse, has a very significant effect on the response. By integrating the waveform file, it was found that the turn-off was not a quarter sine as initially thought, but approximately the last 77% of a quarter sine turn-off. Using a representation of the integrated waveform the simulate the data, the response to the ground model is too low at early times and too high at mid-late times when the time windows as provided by Geotech are used. If the windows are shifted 0.03 ms earlier or slightly more than one sample width of the waveform, then there remains a static 1.15 scale factor between the VTEM model response and data.

The time shift is slightly more than one time sample of the waveform and thus may relate to how the contractor determines the end of the pulse. The amplitude shift, we hypothesize is likely due to how the data is reduced by dipole moment. We have determined a number of possible errors related to this normalization. To properly understand the discrepancy between the ground and VTEM data, more information is required on system parameters.

Overall, our results indicate that MEGATEM and GEOTEM data calibrate with the ground data. They provide relatively deep structural interpretation, but this is still more limited than the depth resolution of the wide-offset ground data. VTEM data may calibrate with the other data, but more information on system settings is needed.

This study highlights the importance of accurately knowing the system parameters such as pulse width, exact window locations and waveform details when trying to determine accurate quantitative geological information.

1.0 Introduction

Airborne TEM is a popular geophysical method in mineral exploration, allowing large areas to be surveyed quickly and efficiently. Airborne TEM has a relatively short history and for many years was used only for qualitative purposes. Today, several different airborne TEM systems

exist, including fixed-wing systems such as MEGATEM and GEOTEM (Fugro Airborne Surveys), and helicopter systems such as VTEM (Geotech Ltd.) and AeroTEM (Aeroquest Ltd.) with in-loop receivers. However, there has been limited work to determine if these data can be used quantitatively in the manner that ground data has been interpreted.

The purpose of our study was to determine if airborne TEM can be used for precise quantitative geological interpretation. If this is possible then if airborne and ground data is collected over the same area, we should be able to develop a model of the ground that corresponds to geology and is consistent for all EM data.

In this study, ground TEM data was used as the basis for the calibration of the airborne TEM. Ground TEM data has been collected for several decades. Modeling codes for ground TEM have existed for some time and have been well calibrated against each other. A model that describes the ground data can be compared with airborne results to determine to what extent they agree. While ground and airborne surveys differ in their resolution, the general structure that they detect should be consistent. We would like to use this calibration site in an attempt to determine the extent of this consistency.

The site selected for the calibration area contains a known breccia pipe. The site underwent extensive study during the 1980's including a variety of historic geophysical surveys and several drill holes. The area was to be an area of intensive study by Uranium One during the uranium boom of the mid-2000's. The entire region was covered by a GeoTEM survey, numerous ground geophysical surveys were carried out by Petros Eikon for Uranium One and all of the geophysical data was studied extensively in attempts to determine how best to detect the breccia pipes via geophysics. Subsequently, some 20 boreholes were sunk in the calibration area in two distinct areas.

All airborne surveys flown for Uranium One's projects in Arizona included a flight over the calibration site for comparison.

1.1 Geologic Setting

The test site is located on the so-called North Rim some distance north of the Grand Canyon, an area that is actively being explored for breccia pipe uranium deposits. The host environment for the breccia pipes is a sequence of sedimentary rocks including limestones, sandstones, and shales as shown in Figure 1. The area is sometimes termed the "Arizona Strip".

At the surface is the Moenkopi Formation, comprised of sandstone and siltstone. Below the Moenkopi are the Kaibab Limestone and Toroweap Formation (predominantly limestone). The Coconino Sandstone, which is quite thin at the calibration site, and the Hermit Shale underlie these. Below the Hermit Shale is a series of formations known as the Supai Group, the uppermost of these formations being the Esplanade Sandstone.

Information on the geology of the area is available from site work by Uranium One just south of the test area. Drill logs extend into the Hermit Shale.

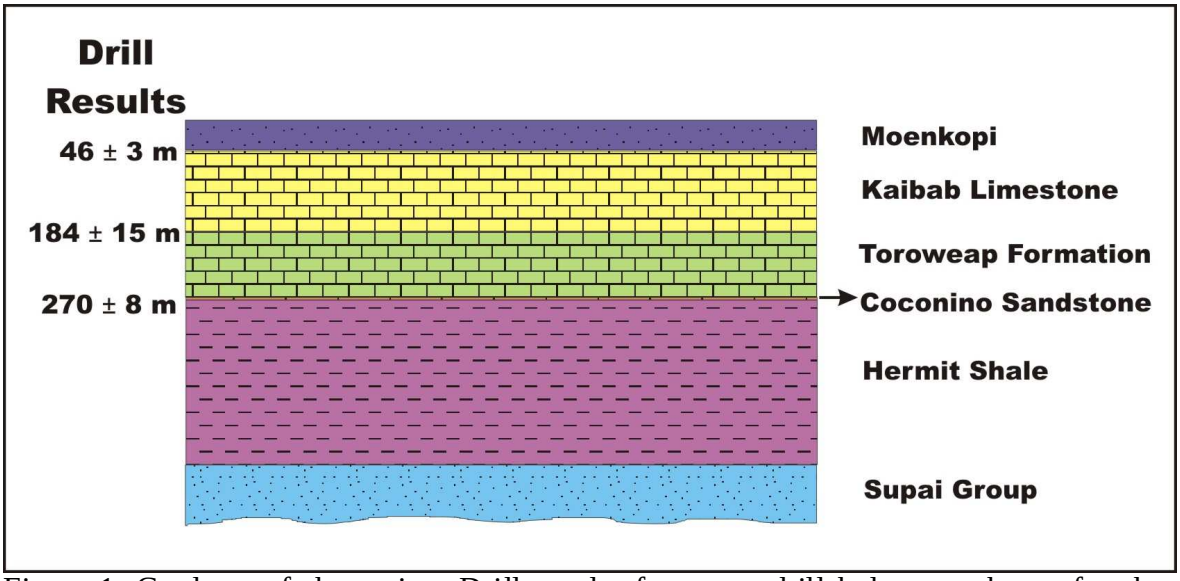

Figure 1: Geology of the region. Drill results for seven drill holes are shown for the upper formations.

1.1.1 Suitability of Site

The geology at this site makes it particularly well-suited for TEM calibration purposes. Firstly, there is little lateral variation in geology at the site. The sedimentary formations are generally flat-lying and there is limited 3D structure. This is seen in the relatively small variation in EM response in the airborne surveys at the site. Therefore, we were able to focus our modeling on layered resistivity models only without concerns as to how the various systems are sensitive to lateral variations. Secondly, although there is limited lateral variation in resistivity, the sedimentary layers have contrasting electromagnetic properties. As a result, we can build a multi-layer model of resistivity versus depth which very accurately represents the resistivity structure. Furthermore, the basement is very deep at this site. If the basement were shallow, we may have only been able to distinguish layering at shallow depths. In contrast, the large thickness of the sedimentary sequence at this site allows us to investigate differences in depth resolution between different surveys.

1.2 Electromagnetic Data

The following data were collected at the test site:

Ground Data:

1. Fixed Loop TEM collected with a PROTEM system using a TEM67 transmitter (Geonics) in May 2008. 400 m x 400 m loop, centered at (750E, 5200N). Data was collected on two long north-south lines (650E and 750E) between 2900N and 6000N at 100 m station spacing. Base frequency was 30 Hz, and all three components were collected.
2. Fixed Loop TEM collected with GDP-32 receiver (Zonge) in May 2008. Same loop as the Geonics survey. Base frequency was 16 Hz. Data was collected only between 5100N and 5800N on Line 650E.

Airborne Data:

1. MEGATEM (Fugro) in February 2007. Base frequency of 30 Hz. Three components. The data was later windowed to have 20 off-time channels rather than the 5 on-time and 15 off-time typically provided. North-south lines at 100 m line spacing. In the vicinity of the test area, the lines are at about 600E, 700E, and 780E, and extend north to about 4900N.
2. GEOTEM (Fugro) in February 2007. Base frequency of 30 Hz, and 20 off-time channels. North-south lines with 100 m line spacing. Two lines have approximately the same easting as the Geonics lines (640E and 740E). GEOTEM was also collected at the test site in 2006.
3. VTEM (GeoTech) in May 2007. Only Hz collected. 28 off-time channels. North-south lines with a line spacing of 100 m. The lines are at approximately the same easting as the MEGATEM lines near the test site (590E, 690E, 790E).

In addition, MaxMin data was collected just 100m south of the calibration area at several frequencies and two separations. VLF-R data was also collected at this site at two polarizations. Several holes were later drilled in the center of these surveys, and drill results extending into the Hermit are available for seven drill holes. The locations of these surveys are shown in Figure 2.

Considerable magnetic data was also collected both from the air and on the ground. This data indicates little shallow magnetic response except for small scale anomalies mostly of man-made origin.

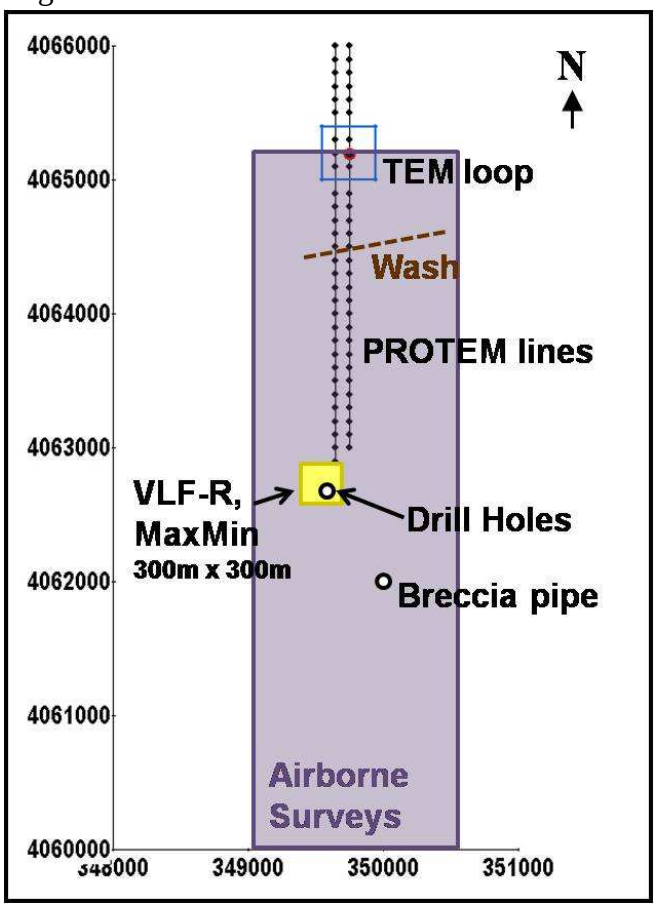

Figure 2: Locations of surveys.

1.3 Method

EMIGMA V8.1 (PetRos EiKon, 2009) was used for layered earth modeling and 1D inversion (Jia *et al*, 2005, Jia *et al*, 2007). The results of the forward modeling code are in agreement with other modeling code in the frequency domain. Comparisons of the time domain response have been performed where possible as well. It should be noted that EMIGMA utilizes a quite different method of determining the time domain response from the frequency domain simulations than other codes. However, this technique has shown itself to be of superior accuracy than other more traditional approaches.

Assessment of the TEM data was performed using the steps outlined below:

1. Development of a layered earth model for the PROTEM ground data:
   A model was developed using a 1D multi-station inversion in which the best model 1D model for several stations was found. The advantage of using a multi-station inversion rather than single-station 1D inversions is that it provides the best overall model, utilizing the different depth resolutions of different receiver locations and limits the ambiguity of the model. Particular attention was paid to both Hx and Hz, including any variation across the survey area, though the ground TEM indicates that the geology is quite uniform laterally.
2. Simulation of the PROTEM ground model for the Zonge system and comparison with the Zonge data.
3. Simulation of the ground model for the MEGATEM, GEOTEM, and VTEM data to determine if the ground data is consistent with the airborne data. Particular attention was paid to ensuring that the correct system settings were used. Waveform files were used to determine these parameters where possible. Finally, a detailed assessment of any discrepancies between the ground data and airborne data was performed. Possible reasons for all discrepancies are considered.

2.0 Ground Data

2.1 Introduction

The geometry of the PROTEM survey was shown in Figure 2. The 400 m x 400 m loop is centered at (750E, 5200N). Data was collected on two north-south lines (650E and 750E) from 2900N to 6000N on Line 650E and 3000N to 6000N on Line 750E. The station spacing was 100m. These lines were chosen so that they were at the same eastings as the GEOTEM lines. The base frequency was 30 Hz, and all three components were collected.

A short line of Zonge data was collected for comparison along 650E from 5100N to 5800N. Three components were collected.

2.2 Modeling Results for PROTEM

2.2.1 Ground Model

Preliminary forward modeling resulted in the development of a four-layer model that has a similar response to the measured data. This model was used as the starting model for a four-layer Marquardt inversion on Hz of the 11 south-most points on Line 650E (1300-2300m south of the loop centre and just off-centre of the loop). Through the use of a multi-station inversion, a single 1D model was developed for these stations. The advantage of using a multi-station inversion is that it provides the best overall model, using the different depth resolutions of different receiver locations. This removes issues with non-uniqueness. The result is Model 4S (Table 1), which fits the data well across the entire survey, as seen in the decay at 3700N in Figure 3. The fact that a single layered resistivity model can be found to generally match the response verifies that the subsurface structure is almost uniform across the survey area and provides an unusual geological sample for these studies. Modeling and inversion work was performed with a 17 kHz upper bandwidth for the receiver. The model is not particularly sensitive to a slightly lower upper bandwidth.

This model was developed by inverting Hz, but the responses of Hx and Hy were also examined. Model 4S fits Hx well, though Hx is generally noisier far away from the loop (Figure 4). Due to the manner in which Hy was collected, the data is not of sufficient quality for interpretation.

Table 1: Model 4S

Resistivity (Ωm)	Thickness (m)	Depth to Bottom (m)	Lithology
123	40	-40	Moenkopi
330	223	-263	Kaibab/Toroweap
40	260	-523	Coconino/Hermit
160			Supai Group

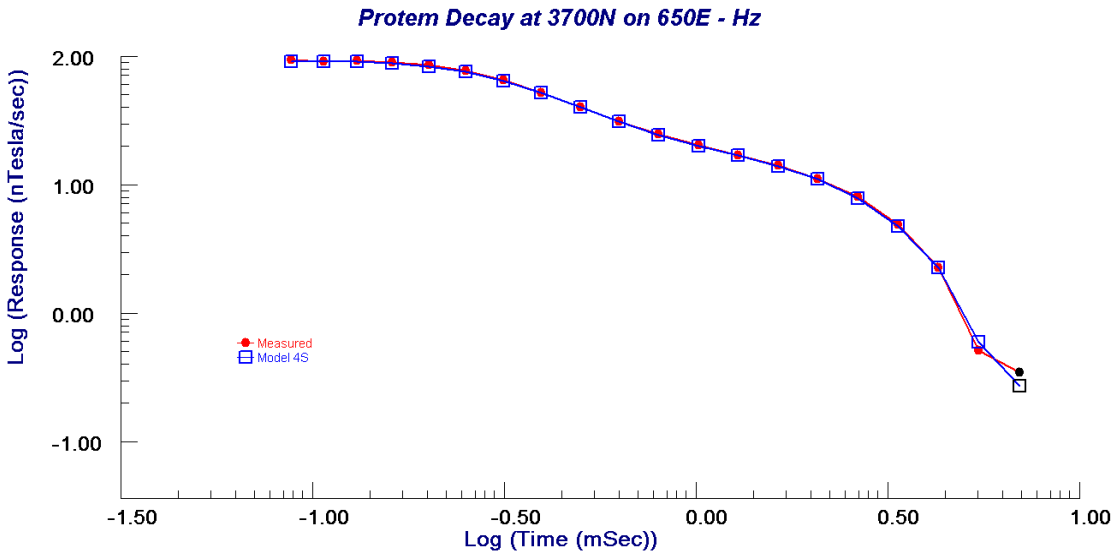

Figure 3: Hz decay at 3700N on Line 650E in the PROTEM ground data. Red is the measured data. Blue is the response of Model 4S.

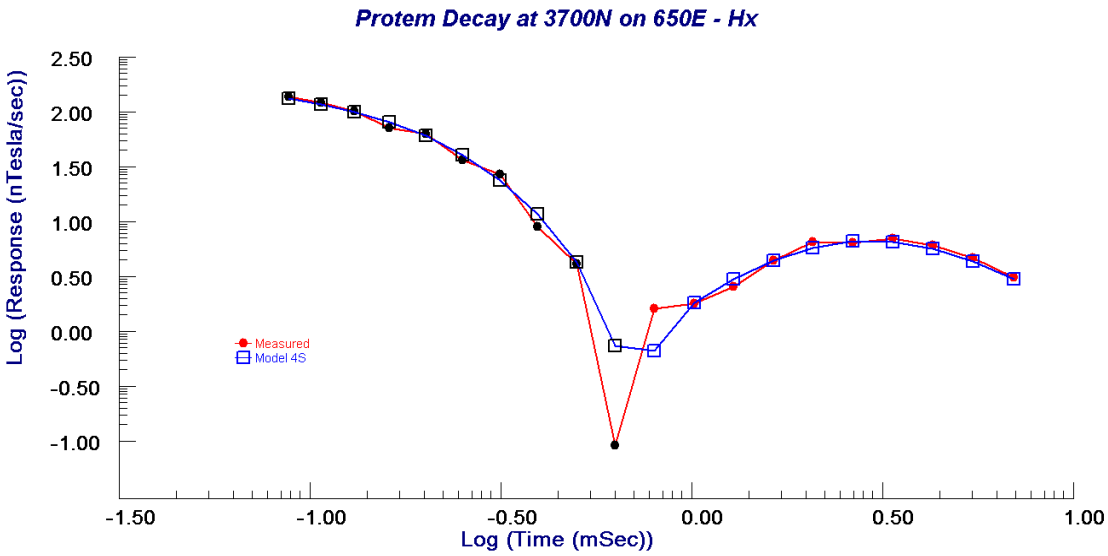

Figure 4: Hx decay at 3700N on Line 650E in the PROTEM ground data. Red is the measured data. Blue is the response of Model 4S.

2.2.2 Comparison with Background Geology

In Table 1, the resistivity structure of Model 4S is correlated with the background geology and in Figure 5, the depths are compared with the drill results. The top layer of 123 Ωm is assumed to be the Moenkopi due to the low resistivity. This resistivity is too low for the limestone-dominated Kaibab and Toroweap, since at other sites in the region where the Moenkopi is absent, EM data shows that there is a much higher resistivity at surface. Both VLF-R and high-frequency Max-Min also have apparent resistivities of about 120 Ωm. Since these methods are not sensitive to deep structure, the apparent resistivity that they detect should be close to the resistivity of the Moenkopi. The VLF-R data does not have significant resolution to determine depth variations in resistivity and the Max-Min data was not of sufficient quality to perform an inversion. The thickness of the Moenkopi in the model (40 m) generally agrees with the thickness of the Moenkopi in the drill cores to the south, where it is 43-50 m thick (46 m average).

The resistive layer below the Moenkopi is the Kaibab and Toroweap. Additional modeling found that these formations cannot be individually distinguished using the EM methods. This is verified in other areas where these structures are at surface.

The 40 Ωm layer beginning at 263 m depth is the Coconino/Hermit. The Coconino is expected to be quite conducting due to saline fluids, but is very thin (about 2 m thick from drill results) in this area. However, we were unable to resolve the Coconino, suggesting that it is not as saline as expected. Even though the Coconino is very thin, if it had the high conductance expected of saline fluids, it could have been resolved based on our modeling results.

The bottom layer is assumed to be the Supai Group (sandstones and siltstones). The drill holes extended only into the Hermit so the depth to the Supai Group in this area is not known. However, the thickness of the Hermit does agree approximately with that observed at a nearby canyon, but we do not have precise information for a comparison.

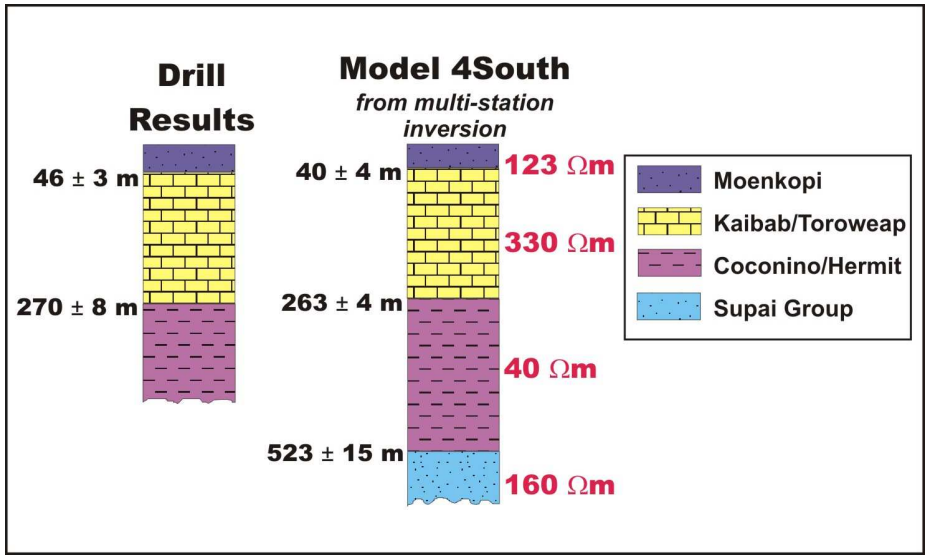

Figure 5: Comparison of drill results with Model 4S from the multi-station inversion on the ground data.

2.2.3 Sensitivity of PROTEM to Supai Group

Each of the four layers in Model 4S is necessary to fit the ground response. However, at short separations, particularly inside the loop, the system is not very sensitive to the resistivity of the fourth layer, or even its existence. For example, if the resistivity of the bottom layer is increased from 160 Ωm to 1000 Ωm, this makes little difference to the in-loop model response (Figure 6a), but has an increasingly larger effect is seen due to the bottom structure when moving away from the loop (Figure 6b). If the Supai Group is removed from the model, there is a slight difference in response for in-loop data at the last eight channels, but a substantial difference in the nature of the decay at large offsets (refer again to Figure 6).

A three-layer Marquardt inversion (not multi-station) in which only the top three layers are in the starting model has good results in-loop but not outside the loop, particularly at large separations. Conversely, a three-layer inversion where only the bottom three layers are in the starting model does not fit the data as well but it is most apparent at early channels inside the loop. This demonstrates the value of using data at different offsets for determining the resistivity structure.

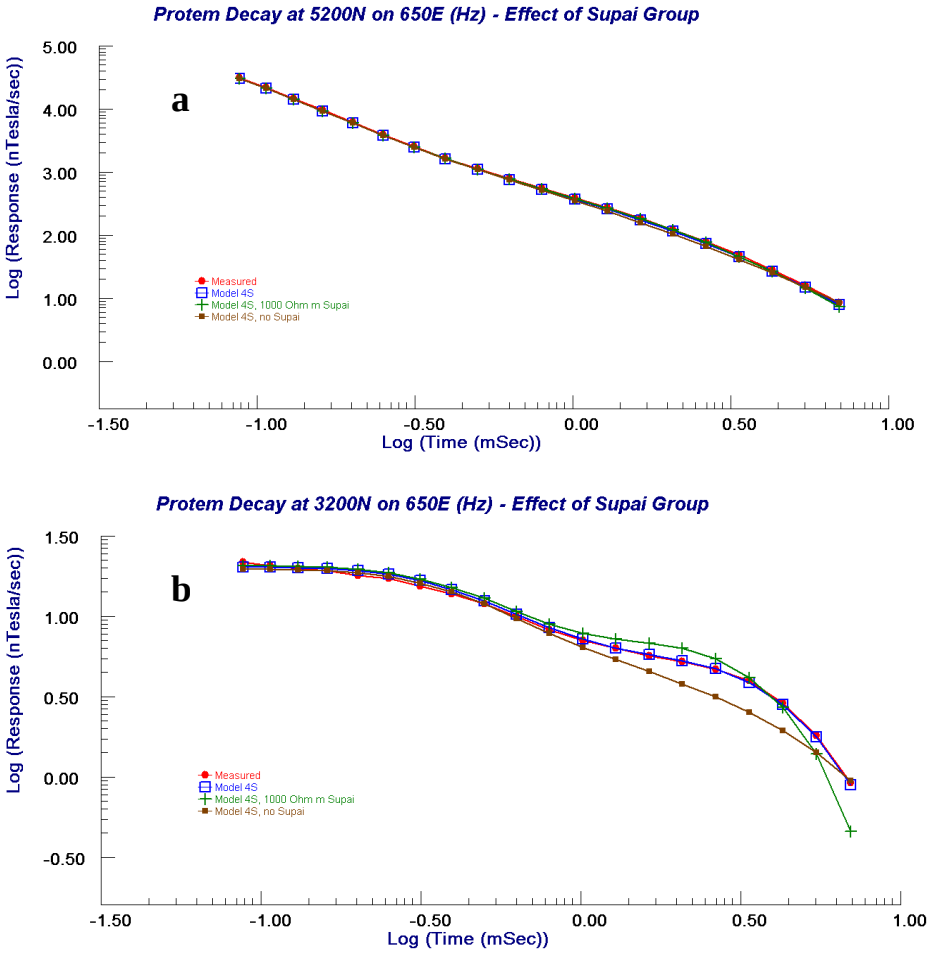

Figure 6: Hz decay at 5200N (a) and 3200N (b) on Line 650E in the PROTEM ground data to show the effect of the Supai Group on the response. Measured data is shown in red and Model 4S is shown in blue. Green is the effect of increasing the resistivity of the Supai Group from 160 Ωm to 1000 Ωm and brown is the effect of removing the Supai Group entirely.

2.2.4 Variation across Survey

While Model 4S fits the data well across the survey, it was noted that near the outside and center of the loop, the response is slightly too low at mid-late times. Decreasing the thickness of the resistive layer by 13 m improves the fit (Model 4N). A decay comparing the response of these two models to the measured data at 4500N is shown in Figure 7. A close inspection of the measured data versus the response of Model 4S and Model 4N shows that there is not a gradual thinning of the resistive layer towards the north, but rather a sudden change at 4400N on 650E and 4300N on 750E in Hz, possibly indicating a fault. This can be observed by comparing the measured data with the models across a profile at late times (Figure 8). Thus, this ground data seems to provide high resolution of somewhat subtler deep structure. This apparent fault corresponds at surface to a wash at about 4400N, as seen in the digital terrain model and observed visually.

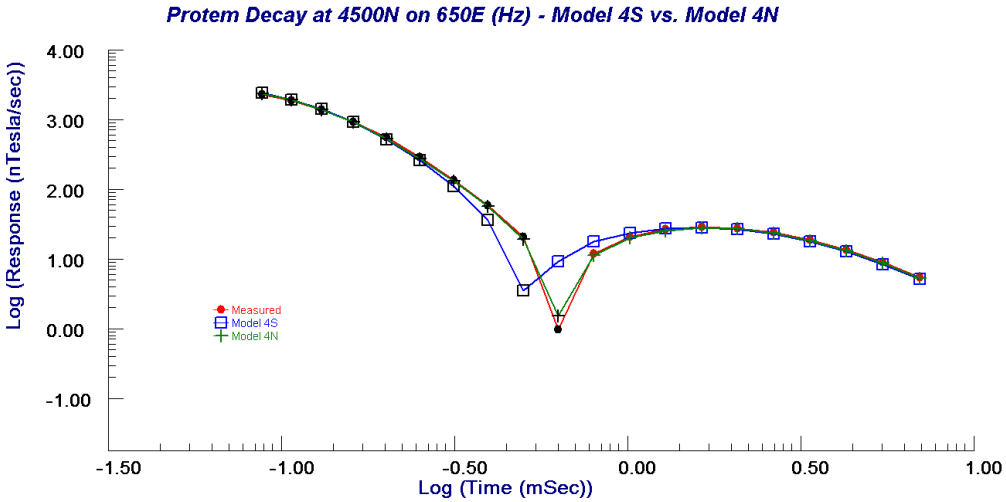

Figure 7: Hz decay at 4500N on Line 650E in the PROTEM ground data. Red is the measured data. Blue is the response of Model 4S, and green is the response of Model 4N.

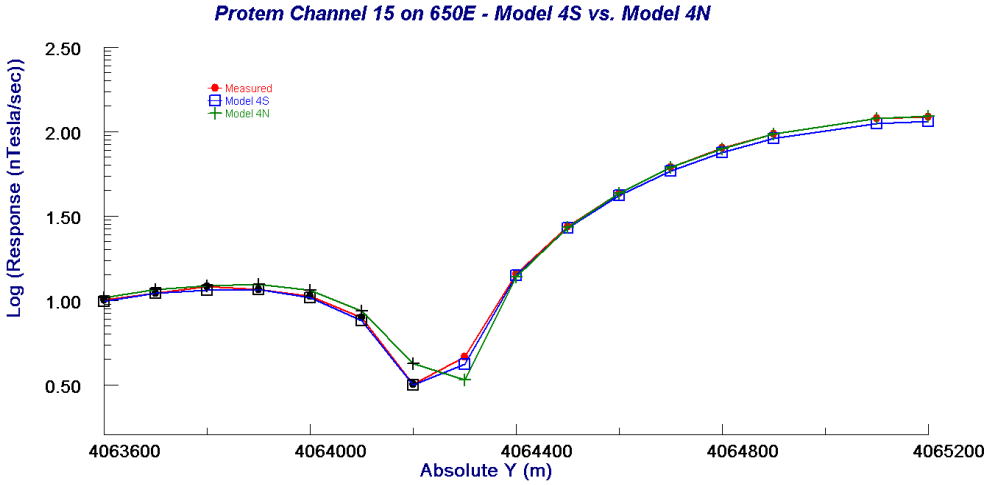

Figure 8: Profile response at channel 15 along a section of 650E in PROTEM ground data. Red is the measured data. Blue is the response of Model 4S, and green is the response of Model 4N.

2.2.5 Reference Cable vs. Crystal Mode

In this study, we have assumed that our settings are correct for the PROTEM data, and taken the PROTEM model as the basis for calibrating the other data. However, analyses of data collected at two calibration stations in different synchronization modes (reference cable and crystal mode) indicate a discrepancy between these two modes (Figure 9). At both stations, the reference cable data is lower than the crystal mode data. If the time positions are shifted 11 μs later, then the REF data matches the XTAL data and the model. This shift between the two modes is consistent with results at a test site in Ontario. This is as of yet an unresolved issue.

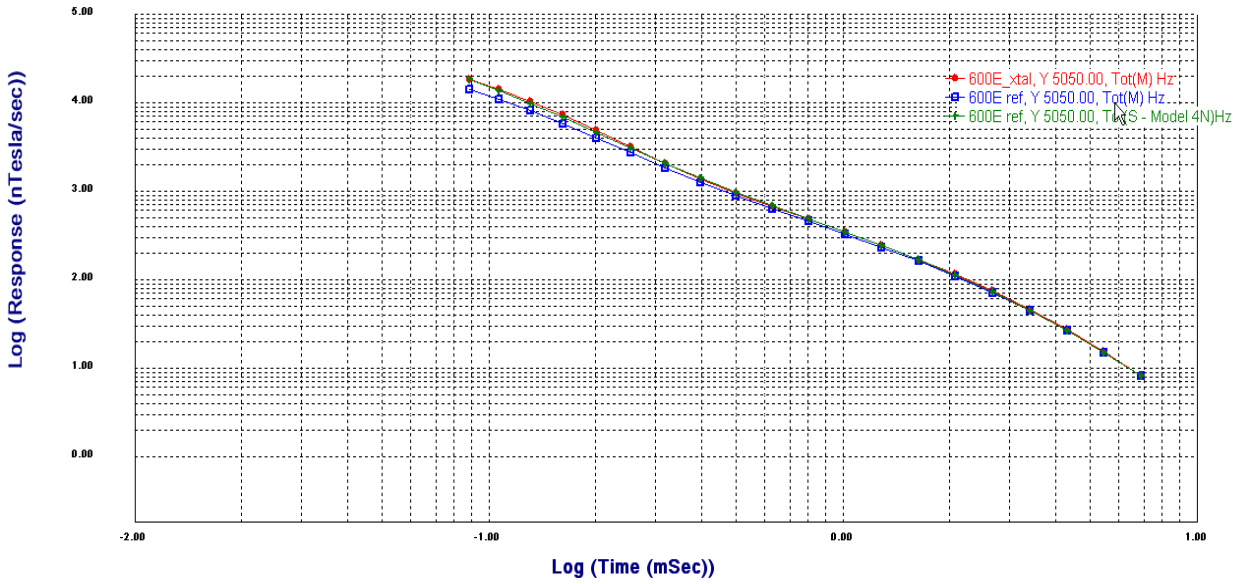

Figure 9: Data at (600E, 5050N). Red is XTAL mode. Blue is REF mode. Green is the response of Model 4N.

2.3 Modeling Results for Zonge Data

According to the GDP-32 manual, the first time channel is determined by subtracting the Tx delay, antenna delay, and antialias delay from the sampling delay. The first time channel is at 0.0337 ms for these data. Model 4N fits the shape of the decay in the Zonge data using these settings, but the amplitude is too small by approximately 15%. When the response of the model is multiplied by 1.15 at all time channels, then the response of Model 4N matches the Zonge data well for all components. These results for the Hz component are shown at the center of the loop in Figure 10.

The cause of this apparent shift factor between the Geonics and Zonge data is not known. It is thought that it could be due to drifting of the current or due to error in reading the current on the instrument. An adjustment in the time channels will not fix this problem, as it will have more effect on the early time channels than on the later time channels. Similarly, shortening the pulse will increase the early time response but will have less effect on the late time response.

With the adjusted amplitude, Model 4S from the south end of the PROTEM survey generally fits the Zonge data too, but Model 4N is a slightly better fit, just as it is a better fit for the PROTEM data near the loop.

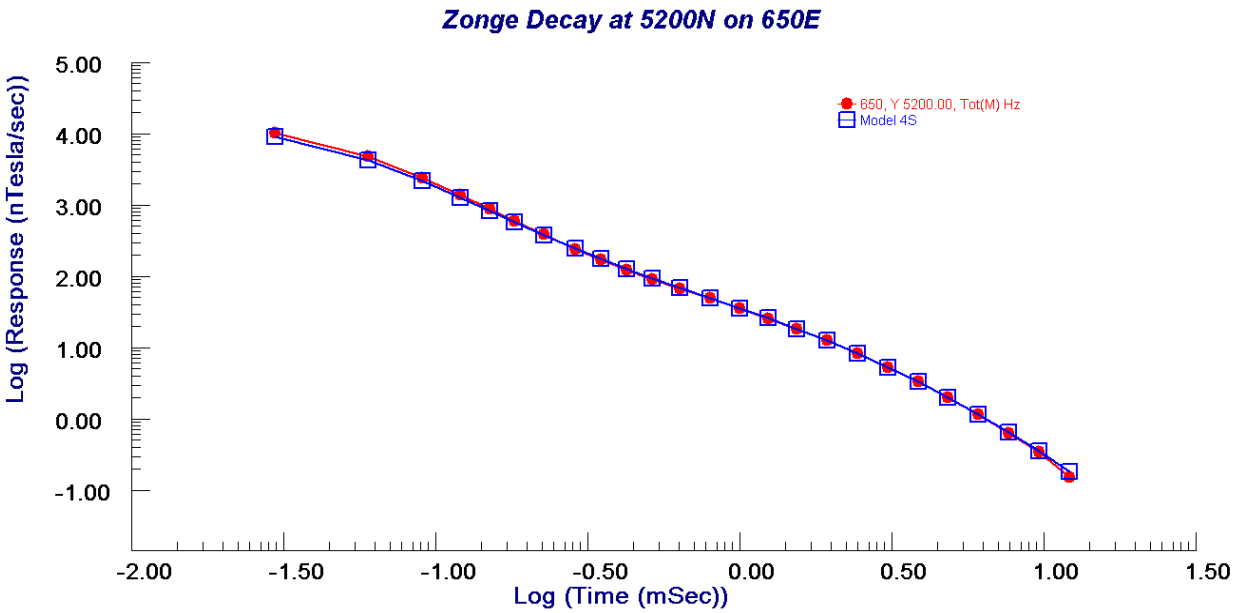

Figure 10: Hz decay at 5200N on Line 650E in the Zonge ground data. Red is the measured data. Blue is the response of Model 4S. Time channels have been shifted and current has been adjusted by 15%.

2.4 Summary of Ground EM data

A multi-station inversion of the PROTEM data resulted in Model 4S, which fits the measured data well across the survey and corresponds with the geology. The survey is sensitive to the Supai Group below the Hermit although drill holes did not extend beyond the Hermit. This layer is required to match the shape of the decay at large offsets, though at short separations, the response was not very sensitive to it. While a single model is a reasonable fit across the survey, there appears to be some variation, with a slightly shallower depth to the Coconino north of 4300N.

It was found that the Zonge data is in agreement with the PROTEM provided the time channels are adjusted, but there is a small (approximately 15%) issue with the amplitude of the data. However, we have yet to determine if these adjustments are reasonable for the system.

3.0 MEGATEM

3.1 Introduction

MEGATEM data with a base frequency of 30 Hz was collected over a large survey area south of the Grand Canyon, but data was collected over the calibration site for comparison with the ground data and other airborne data. The line spacing was 100 m. Station spacing was approximately 13 m. Although three components were collected, we focused on Hz as it had the cleanest decays.

While the original data had 5 off-time channels and 15 on-time channels, it was later windowed such that it had 20 off-time channels, with increased channel density in early and mid-times. The purpose of the re-windowing was to provide increased shallow resolution and remove ambiguities with the mid-time data. The re-windowing was critical for interpreting the data.

3.2 System Settings

A waveform file was provided for each flight in the MEGATEM survey including the flight containing the calibration site. The waveform files contain the dipole moment and the response of each of the three coils (dB/dt as well as B) collected at high altitude. This corresponds to the freespace response for the system, as the system is not sensitive to the ground at high altitude. Spectral analyses were done of the high altitude data to determine the power spectrum of the data.

The waveform files were used to determine the pulse width and dipole moment. Additionally, the waveform files list the samples that correspond to each time window. Combined with the sampling interval, this allowed the times of the windows to be checked.

A further use of the waveform files was for checking the geometry of the system. The freespace response can be simulated and compared to the waveform files. As the waveform specifications and dipole moment were known, this allowed us to check the transmitter-receiver separations. Fugro had stated that the receiver was 128 m behind the transmitter and 62 m below it. However, from comparing the amplitude of the simulated freespace response for dBz/dt and dBx/dt with the waveform files, it was determined that the separation in x was correct but the separation in z was not. The simulated dBz/dt for the given separations was about half as large as that in the waveform file. Decreasing the separation in z increases the freespace response. It was found that a separation of 46 m was more appropriate than 62 m. Furthermore, some of the rewindowed data files contain transmitter-receiver offsets for each data point as estimated by Fugro. The vertical offset is typically 45-50 m and there are only a few lines in which it is above 60 m. This corresponds to the offset determined from modeling the freespace response. Unfortunately, offsets are not given for each point for the calibration site data.

3.3 Simulation Comparisons of Ground Model to MEGATEM data

3.3.1 Initial simulation

Model 4S was simulated for the MEGATEM data over the calibration test area after carefully checking pulse width, dipole moment and window positions. The focus was on Line 10090, which is in between the two ground survey lines. Initially, we utilized a bandwidth up to 17 kHz. Although Model 4S matches the MEGATEM data at mid-late times reasonably well, the response of the model is too high at the first time channel and too low at subsequent early channels (Figure 11). It was not possible to find a reasonable model without adjusting the upper frequency of the system bandwidth. The model required to fit with the upper frequency at 17KHz

includes a thin very resistive layer at the surface. This shallow resistivity model is not physically possible and contradicts all the ground EM data.

The MEGATEM data also shows a variation in response from north to south over the calibration site that was not observed in the PROTEM data. From 4200N to the north end of the survey, the early-time response is fairly constant whereas the early-time response continually increases from 4200N to the south end of the calibration site.

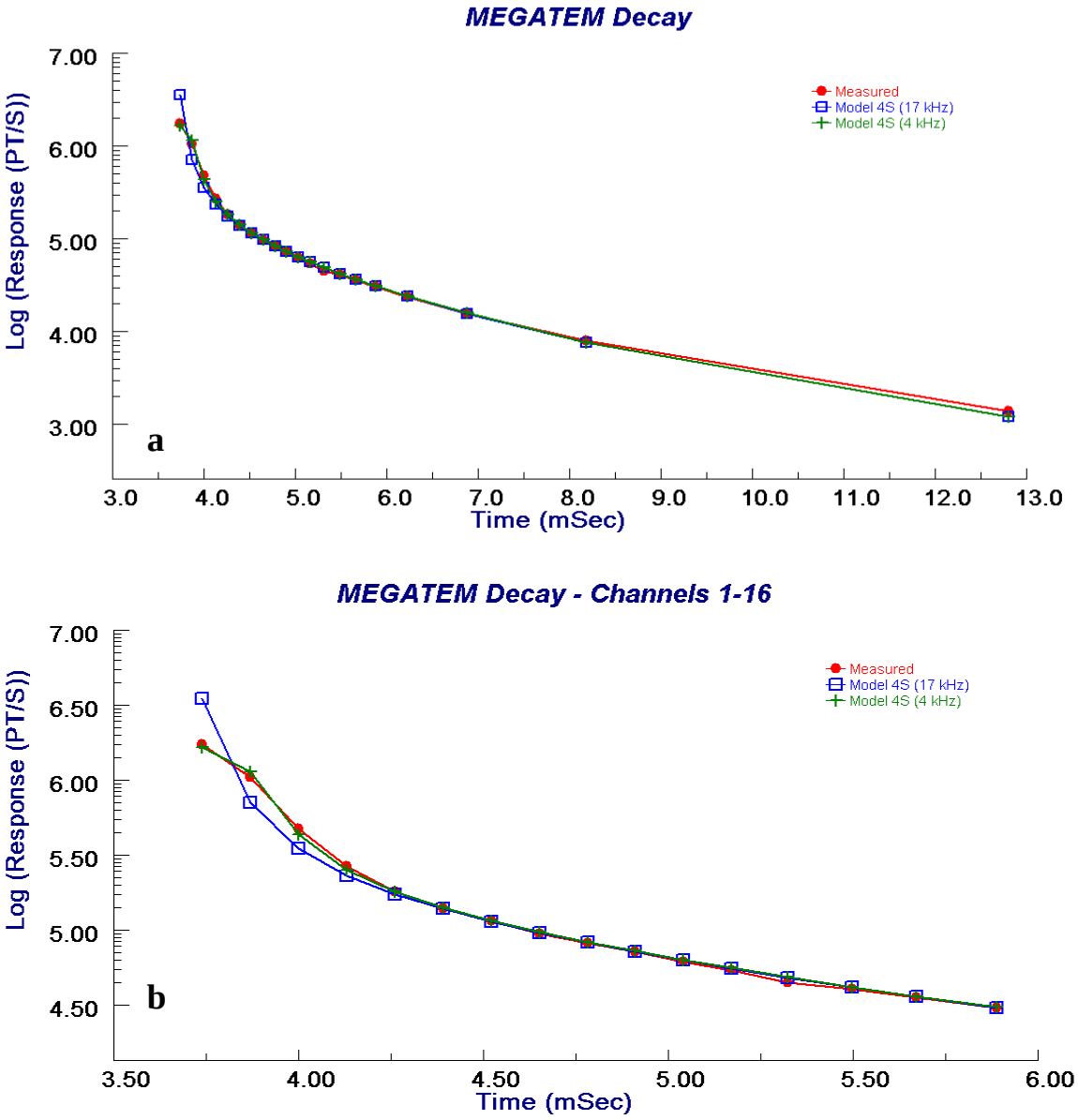

Figure 11: Hz decay on Line 10090 at (700E, 4360N) in the MEGATEM. Red is the measured data. Blue is the response of Model 4S for a receiver bandwidth of 17 kHz. Green is the response of Model 4S for a receiver bandwidth of 4 kHz. a) is the decay at all channels and b) shows only channels 1-16 to focus on the early-mid times.

3.3.2 Bandwidth Adjustment

The initial simulation of Model 4S for the MEGATEM was performed using an upper bandwidth of 17 kHz for the system with a low-pass filter applied. If a bandwidth limited to 4 kHz is used instead of 17 kHz, the Model 4S fits the MEGATEM data well to the north of 4200N where the response stays constant (Figure 11). However, after this adjustment in bandwidth the response of the model south of 4200N is slightly too small but just for the early channels. This misfit increases until it reaches a maximum at station 3000N (Figure 12). Mid-time and late-time still fit. This increase in response to the south is also observed in the GEOTEM and VTEM.

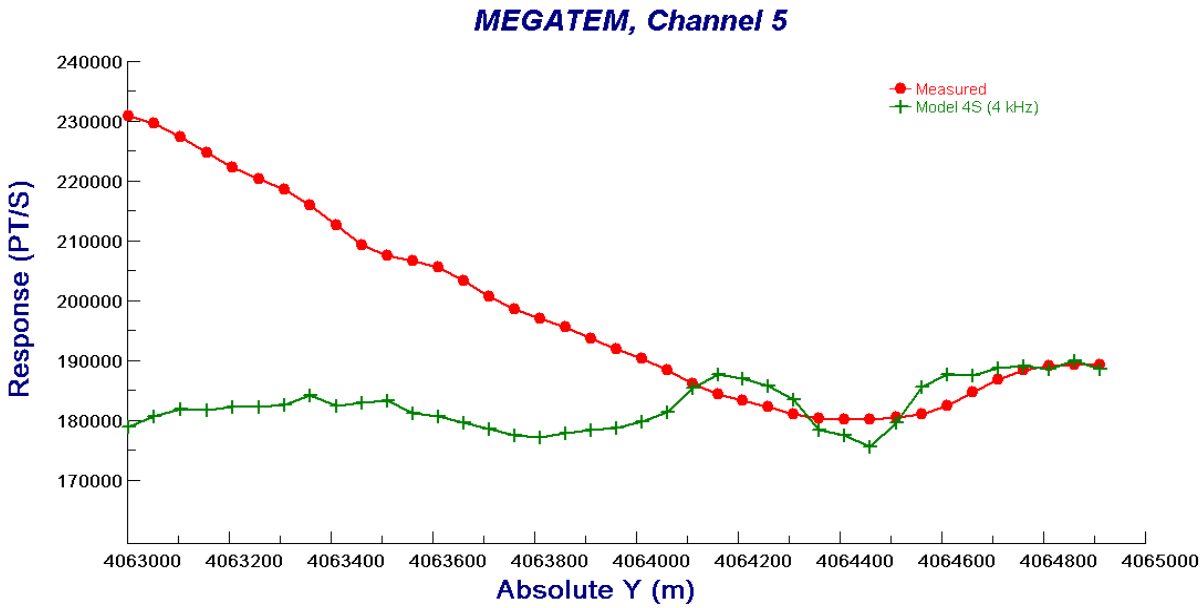

Figure 12: Comparison of measured MEGATEM Hz data (red) with Model 4S simulated at 4 kHz (green) for channel 5 along Line 10090. An increase in response to the south is observed in the measured data.

3.4 Comparison with Ground Results

3.4.2 North-South Variation

To adjust the model to fit the increasing amplitude of the early channels at the south end of the survey requires adding some shallow conductance of about 0.25S. This increased conductance could be provided by several factors: a decrease in the resistivity of the surface layer (Moenkopi), an increase in thickness of the surface layer or an additional thin conducting layer near surface. The MEGATEM survey does not have sufficient shallow resolution to distinguish between these possibilities. However, analyses of other data suggest that some of these factors are unlikely. A decrease in the resistivity of the surface layer is ruled out by the VLF-R and MaxMin data collected just south end of the site in an area also covered by the airborne data. Both these surveys show conclusively that this increased conductance cannot be near surface. Also, physically there is no reason for very shallow decreased resistivity as there is little moisture at surface and high temperatures and a very arid environment causes rapid evaporation of any moisture from the shallow materials. An increase in the thickness of the Moenkopi is ruled out by the drill cores obtained from several drillholes 100m south. The only remaining

possibility from a geological perspective is the possibility of a deeper layer of lower resistivity within the Moenkopi or at its base.

It is possible that the PROTEM survey would not be sensitive to a conductive layer within the Moenkopi at the south end of the survey as the receivers are far from the loop and the currents have migrated to some depth by the time they reach the south end. To examine this, we placed a plate of 0.25 S within the Moenkopi in Model 4S and simulated the response. While this simple model does not match the MEGATEM across the entire line, it is a reasonable fit to the south from 3200-3700N (Figure 13a). This model was then simulated for the PROTEM system. The response to this model varies somewhat from the response to Model 4S at early times. At two stations it appears that this model may be slightly better than Model 4S; however, the early time PROTEM data is noisy at large offsets from the loop so it is difficult to draw conclusions (Figure 13b). Thus, a model with additional conductance within the Moenkopi to the south, which better fits the MEGATEM, would not be inconsistent with the ground data.

The variation in MEGATEM response is observed not only on Line 10090, but on other lines at the calibration site. Single station 1D inversions were performed on all stations of the MEGATEM data on Lines 10010-10210 from 4063000 north to the end of the survey. The results are fairly consistent across the survey, as shown in Figure 14. However, an increase in conductance to the south is visible on all lines.

3.4.1 Comparison of North and South Ground Models

The initial model developed for the ground data was Model 4S, which is from a multi-station inversion on the south portion of Line 650. It was later found that decreasing the thickness of the limestone by 13 m improved the fit with the stations from 4400 north: this is Model 4N.

Initially the south model for the ground data, Model 4S, was simulated for the MEGATEM and it was found to match the MEGATEM north of 4200N provided that a bandwidth of 4 kHz was used. However, at the north end of the calibration site, Model 4N better fit the ground data better than Model 4S. Therefore, Model 4N was simulated for the MEGATEM to the north to determine if it fit better than Model 4S. It was found that Model 4N had a greater mid-late time response than Model 4S for the MEGATEM due to the shallower depth to the 40 Ohm m layer. This produced a poorer fit to the measured data (Figure 15). Therefore, the MEGATEM suggests a greater depth to the Coconino north of the wash than the PROTEM. Or more simply, the MEGATEM apparently does not see the apparent fault at the wash.

One possibility is that this is due to there being an offset between the MEGATEM lines and the ground lines, and there is some east-west variation over the site. The MEGATEM lines are spaced every 100 m and Line 10090 is at 700E, in between the ground survey lines at 650E and 750E. However, the two ground lines show consistent results. Furthermore, adjacent MEGATEM lines have a similar response to Line 10090. Therefore, it is unlikely that a change in geology could explain the fact that Model 4S fits the north part of the MEGATEM better than Model 4N. This suggests a slight discrepancy between the MEGATEM and PROTEM data. It should be noted, however, that in the MEGATEM, the difference between these models is relatively small: 5-6% at mid-late times. In contrast, the difference between the responses to these two models at some receivers in the ground survey is more significant.

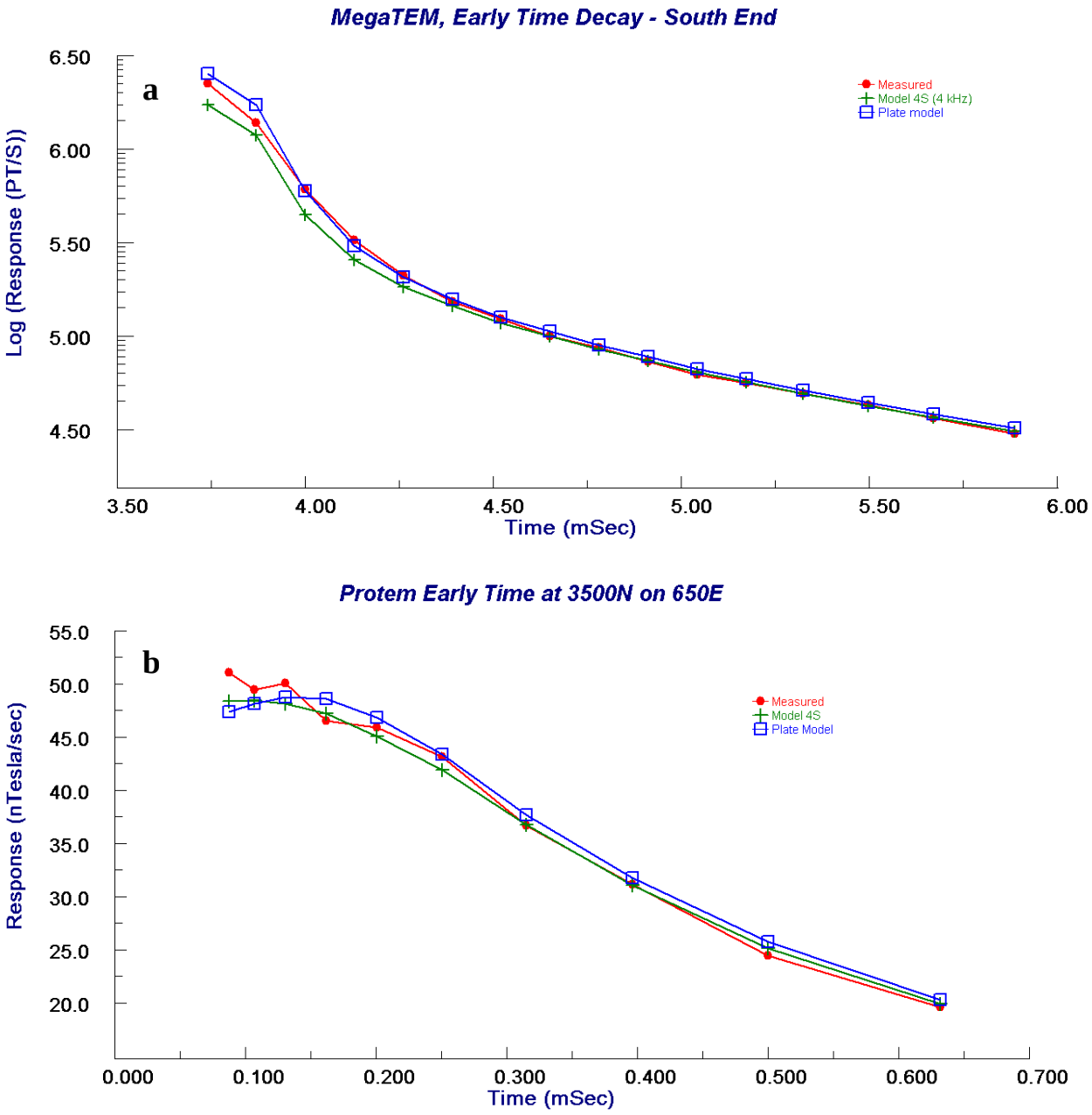

Figure 13: a) Comparison of measured MEGATEM Hz data (red) with the simulated response for Model 4S (green) and the plate model (blue) on Line 10090 at (700E, 3461N) at early-mid times. b) Comparison of PROTEM data with the same models at early time on Line 650E at 3500N.

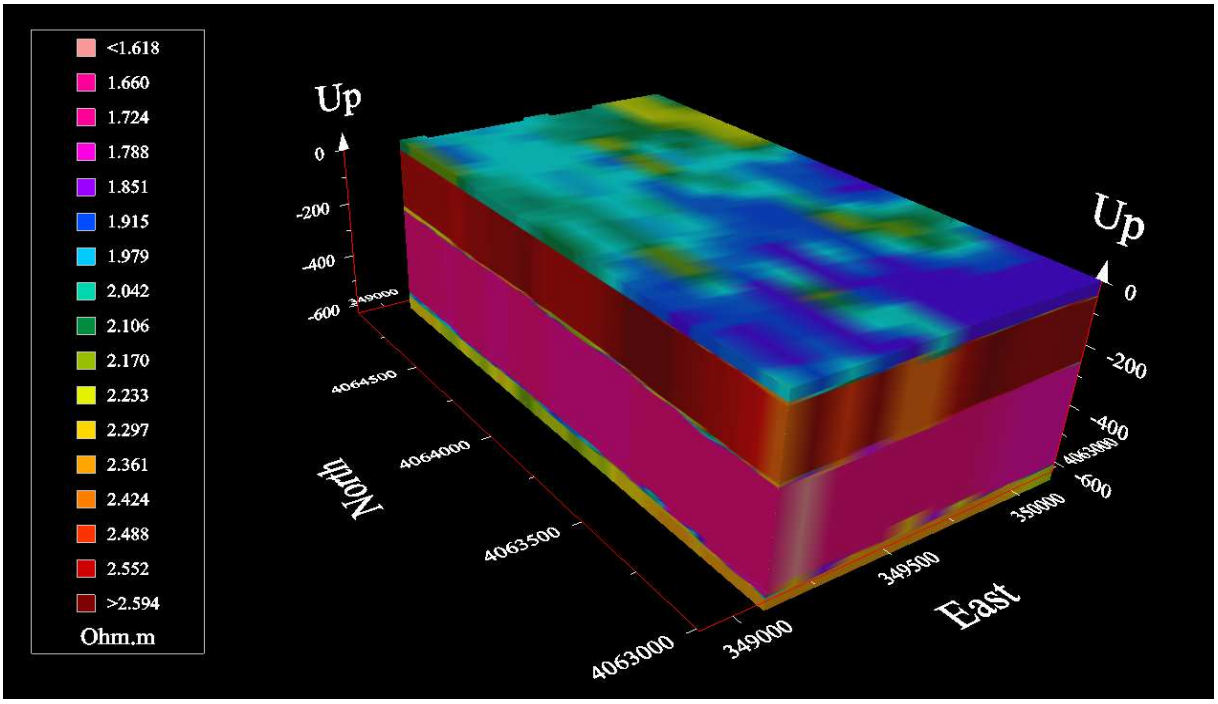

Figure 14: 3D visualization of 1D MEGATEM inversions from 349100-350200 E and 4063000-4065000 N.

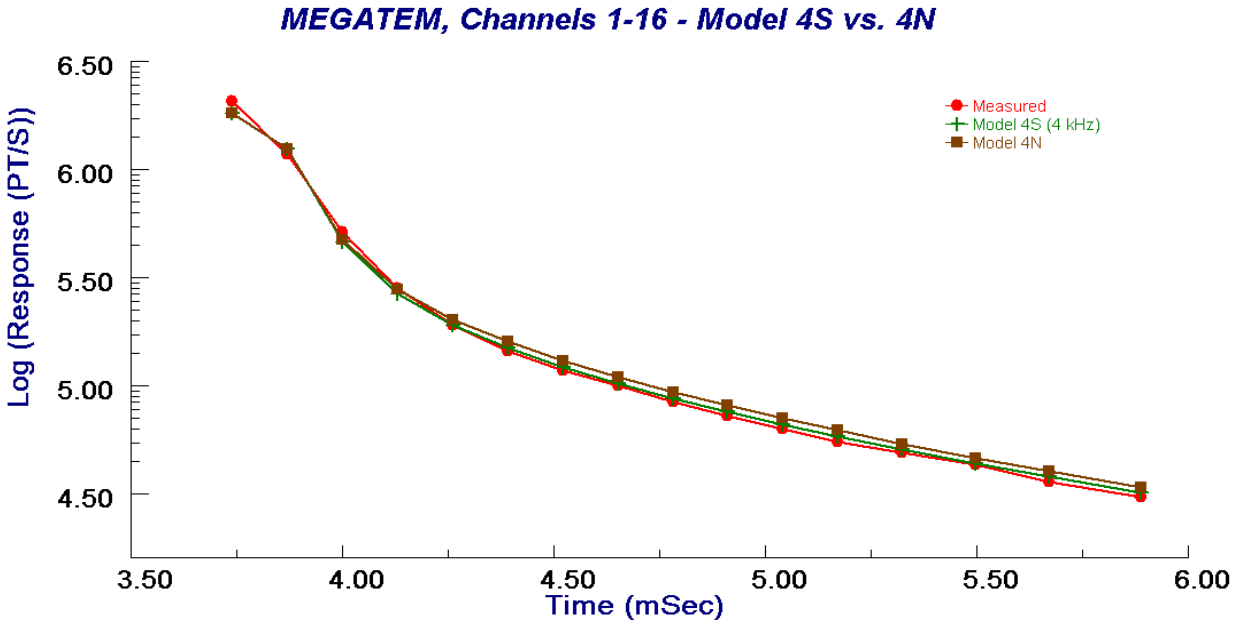

Figure 15: Comparison of measured MEGATEM Hz data (red) with the simulated response for Model 4S (green) and Model 4N (brown) on Line 10090 at (700E, 4812N) at early-mid times.

3.4.3 Sensitivity of MEGATEM to Coconino/Hermit and Supai Group

As noted, the difference in depth to the Coconino between the two ground models results in a very small difference in response for the MEGATEM. We also examined the effect of removing the Supai Group from the model and also experimented with adjusting the resistivity of the Supai and the effects on the MEGATEM response.

It was found that removing the Supai Group from the model by assuming the Hermit continued indefinitely had a limited effect at early times but decreased the response at later channels (Figure 16) as compared to the measured data. The difference increased gradually to a maximum of about 14% at Channel 17. This shows that the MEGATEM has some sensitivity to the geology at this depth. It also gives strength to the accuracy of the MEGATEM data at late times. We among others have often been nervous about the effects of the Fugro late-time filtering.

In the ground model, if we replace the Coconino/Hermit and Supai Group with one structure of 28 Ωm then the modified model fits the data as well as the original model. If the resistivity of the Hermit is known, then the inversion of the MEGATEM does indicate the Supai Group although the depth and resistivity of this structure are somewhat different from the PROTEM model.

The Supai Group has some effect on the MEGATEM response but the MEGATEM cannot be used to determine the depth to the Supai. In contrast, the PROTEM system was very sensitive to the Supai Group (2.2.3).

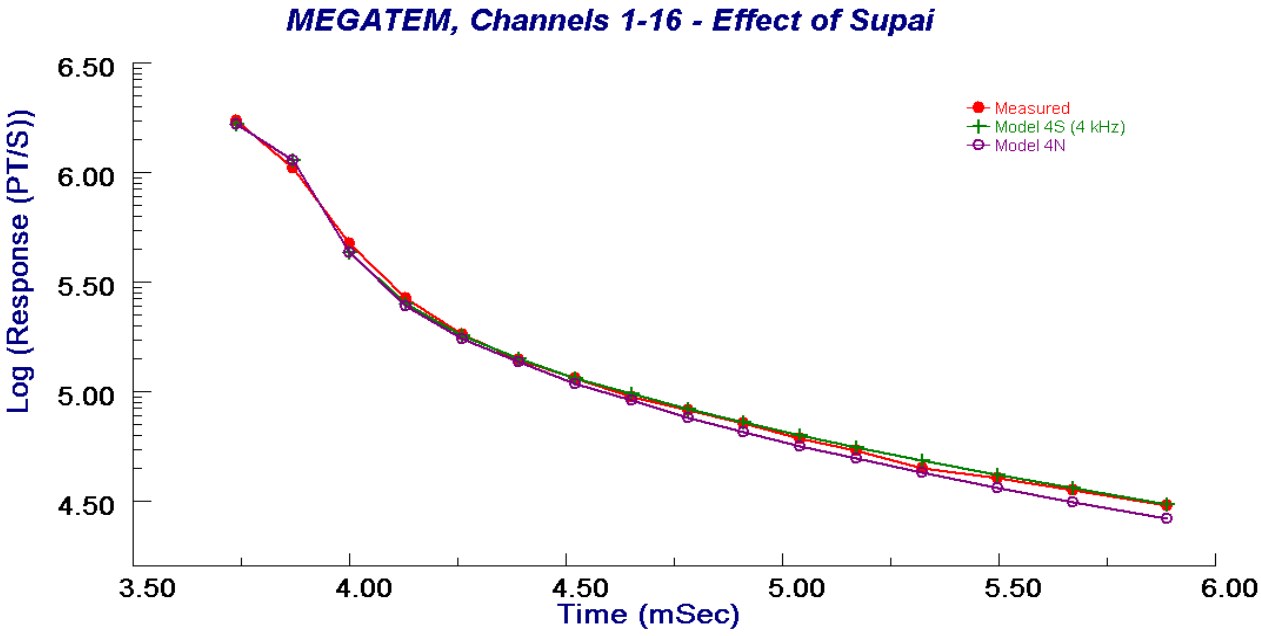

Figure 16: Comparison of measured MEGATEM Hz data (red) with the simulated response for Model 4S (green) and Model 4S without the Supai group (purple) on Line 10090 at (700E, 4360N) at early-mid times.

3.5 Summary

The MEGATEM data at the calibration site agrees quite well with the PROTEM data north of 4200N provided that an upper frequency for the system bandwidth is set at 4 kHz. The MEGATEM data suggests a slightly greater depth to the Coconino north of 4200N (wash) than the PROTEM. However, this is a fairly small discrepancy.

The MEGATEM shows an additional shallow conductance towards the south, unlike the PROTEM data. Presumably the ground data would not be very sensitive to this shallow conductance away from the loop. Modeling studies support this hypothesis.

3.5 Summary

The MEGATEM data at the calibration site agrees quite well with the PROTEM data north of 4200N provided that an upper frequency for the system bandwidth is set at 4 kHz. The MEGATEM data suggests a slightly greater depth to the Coconino north of 4200N (wash) than the PROTEM. However, this is a fairly small discrepancy.

The MEGATEM shows an additional shallow conductance towards the south, unlike the PROTEM data. Presumably the ground data would not be very sensitive to this shallow conductance away from the loop. Modeling studies support this hypothesis.

4.0 GEOTEM

4.1 Introduction

GEOTEM data was collected over a large area that included the calibration site. Line spacing was 100 m and station spacing was 13 m. The base frequency was 30 Hz. The original data had 5 off-time channels and 15-on time channels. As with the MEGATEM, the data was rewindowed to have 20 off-time channels such that there was increased channel density at early-mid times. The rewindowing was essential for quantitative interpretation of the data.

4.2 System Settings

A waveform file was provided for each flight in the GEOTEM survey. Each waveform file contains the dipole moment and the response of each of the three coils (dB/t and B) collected at high altitudes. The waveform file for the flight over the calibration site was used to check dipole moment, pulse width, and time windows.

The waveform file was also used to check system geometry. The freespace response was simulated and compared with the high altitude response. Unlike the MEGATEM, the geometry provided by Fugro for the GEOTEM is consistent with the waveform files.

4.3 Simulation of Ground Model

4.3.1 Initial Simulation

Similar to the MEGATEM, Model 4S fits the GEOTEM well at mid- to late times when a bandwidth of 17 kHz is used. However, the model does not fit the data well at early times (Figure 17). The GEOTEM data also has an increase in early-time response south of 4200N, reaching a maximum at the south end of the site (3000N).

4.3.2 Bandwidth Adjustment

When the upper bandwidth is decreased to 6 kHz, Model 4S fits the data north of 4200N (wash) where the response is nearly constant (Figure 17). This is greater than the 4 kHz bandwidth used for the MEGATEM. At additional sites in the area for which both GEOTEM and ground data were available, and it was found that an upper bandwidth of 6 kHz produced excellent comparisons between the GEOTEM and PROTEM models.

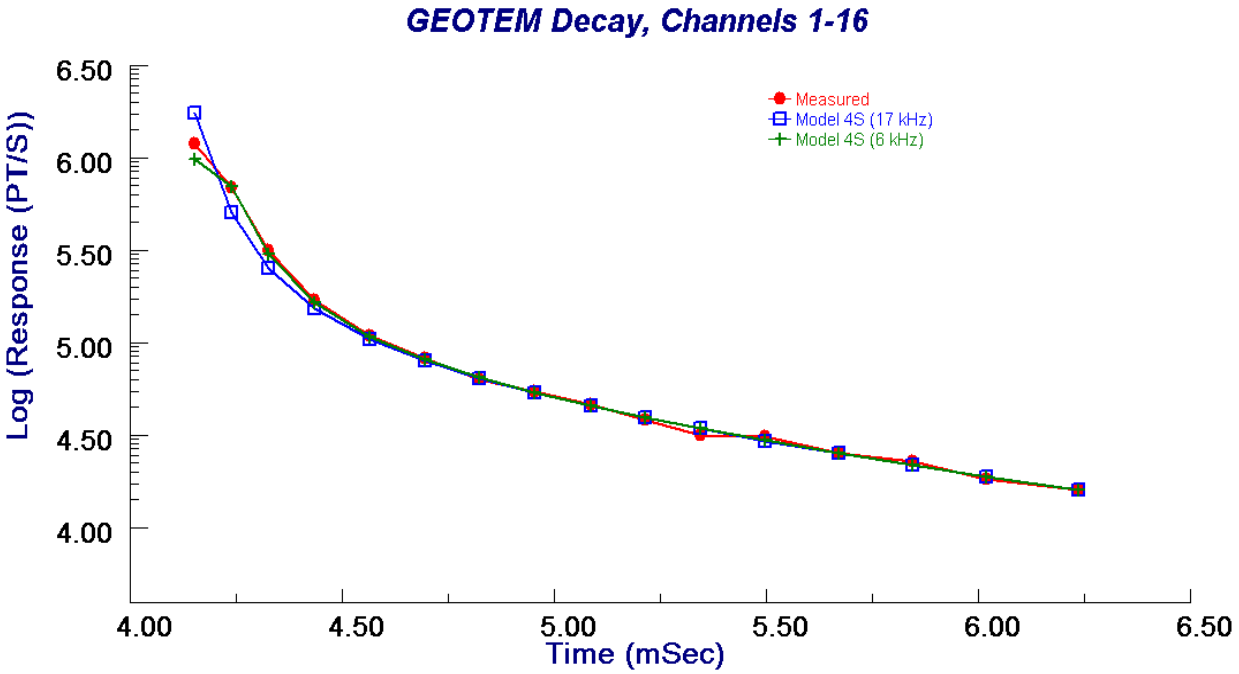

Figure 17: Comparison of measured GEOTEM Hz (red) with the simulated response for model 4S at 17 kHz bandwidth (blue) and 6 kHz bandwidth (green) at 4330N on Line 12440.

4.3.3 Comparison of MEGATEM and GEOTEM Bandwidth

For the ground model to fit the MEGATEM, an upper bandwidth of 4 kHz was needed and for the GEOTEM, a bandwidth of 6 kHz was needed. These bandwidths were determined by simulating the model response at several different bandwidths and determining which was the

best fit to the data. In addition, these bandwidths were relatively consistent with spectral analyses of the waveform files.

To further study the bandwidth of these systems, we modeled the freespace response at several different bandwidths and compared the results with the waveform files for each system. We looked at 20 time samples of dBz/dt centered at the end of the pulse. When the signal is turned off, dBz/dt goes from a minimum (a large, negative value) eventually to zero (Figure 18). However, this does not occur instantaneously due to bandwidth limitations and filter effects.

It is clear from this work that 17 kHz is much too high for an upper bandwidth for both systems. For the GEOTEM waveform, a bandwidth of 6 kHz very closely approximates the dBz/dt seen in the waveform files (Figure 19). For the MEGATEM, the response appears less symmetrical: the response just before the end of the pulse suggests a higher bandwidth than the response just after the end of the pulse. A bandwidth of 4 kHz fits the response well by 0.2msec after the end of the pulse (Figure 20). The reproduction in EMIGMA of the low pass filtering effects seems well reproduced for the GEOTEM but not so well in the MEGATEM. However, for the time windows utilized the reproduction is adequate.

According to Fugro, both MEGATEM and GEOTEM systems use the same coils with the same bandwidth (J. Lemieux, personal communication, 2007). However, modeling work at the calibration site, it seems that these two systems have different bandwidths. Also, modeling of the waveforms and spectral analyses indicates the same result. However, the bandwidth is not determined simply from the receiver coils. There are differences between the systems that may be the cause of the lower bandwidth for the MEGATEM. The MEGATEM has a greater dipole moment, which results in greater responses. According to Fugro, the MEGATEM takes 0.1 ms longer to return to zero following the end of the pulse as a result (J. Lemieux, personal communication, 2007).

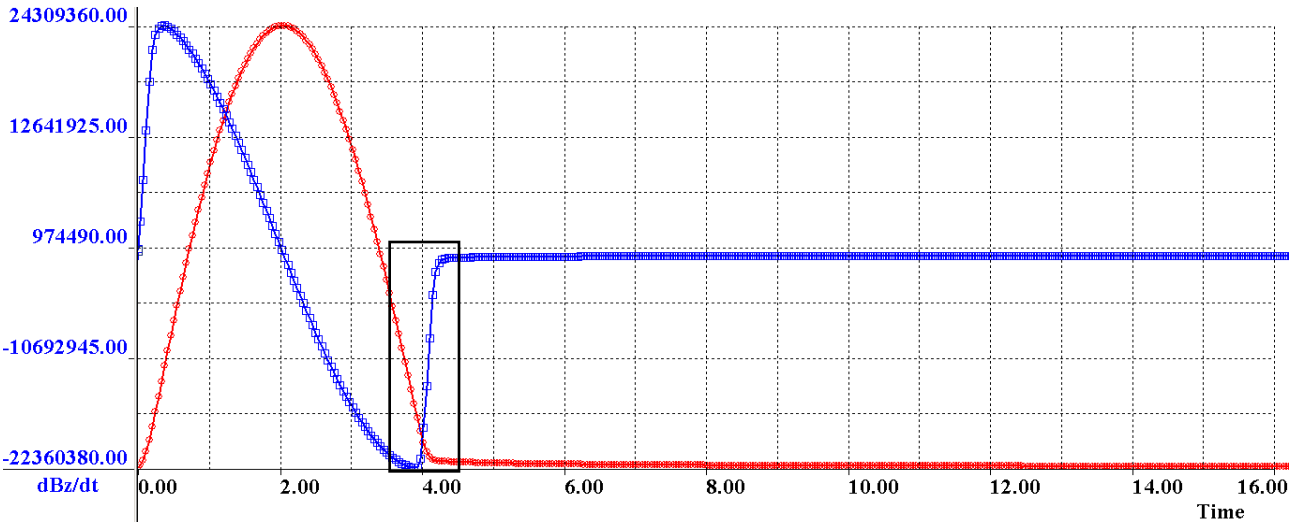

Figure 18: Comparison of Bz and dBz/dt in a GEOTEM waveform file. Y-axis scale is shown for dBz/dt. The section of dBz/dt in the box is what is shown in Figure 20.

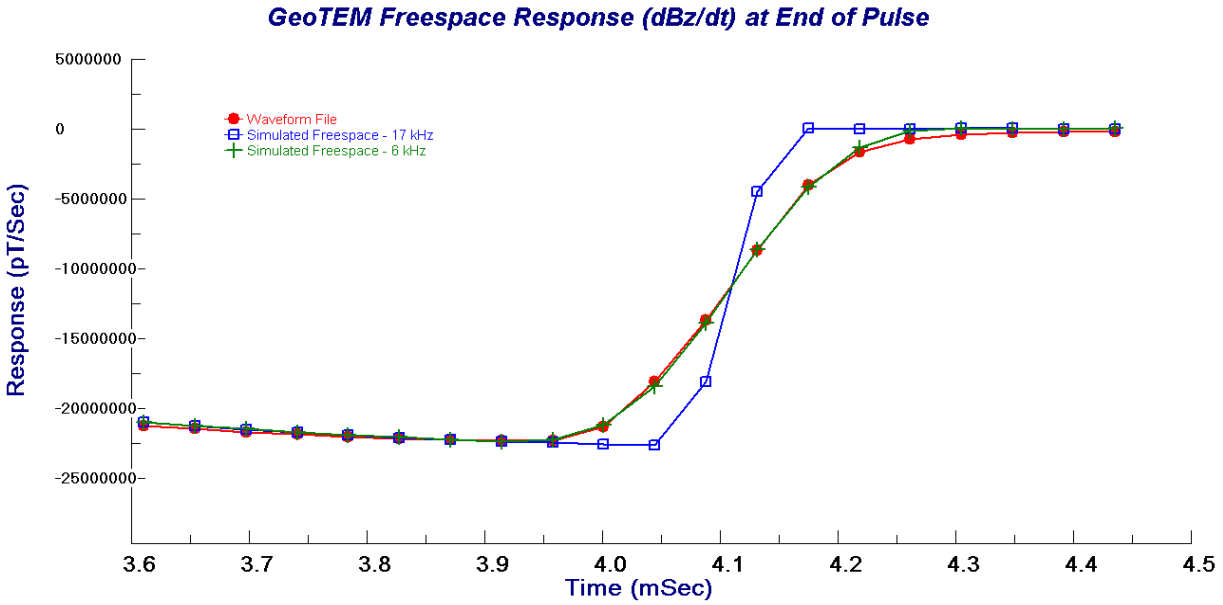

Figure 19: Comparison of dBz/dt at the end of the pulse for a GEOTEM waveform file (red) and the simulated freespace response for upper bandwidths of 17 kHz (blue) and 6 kHz (green).

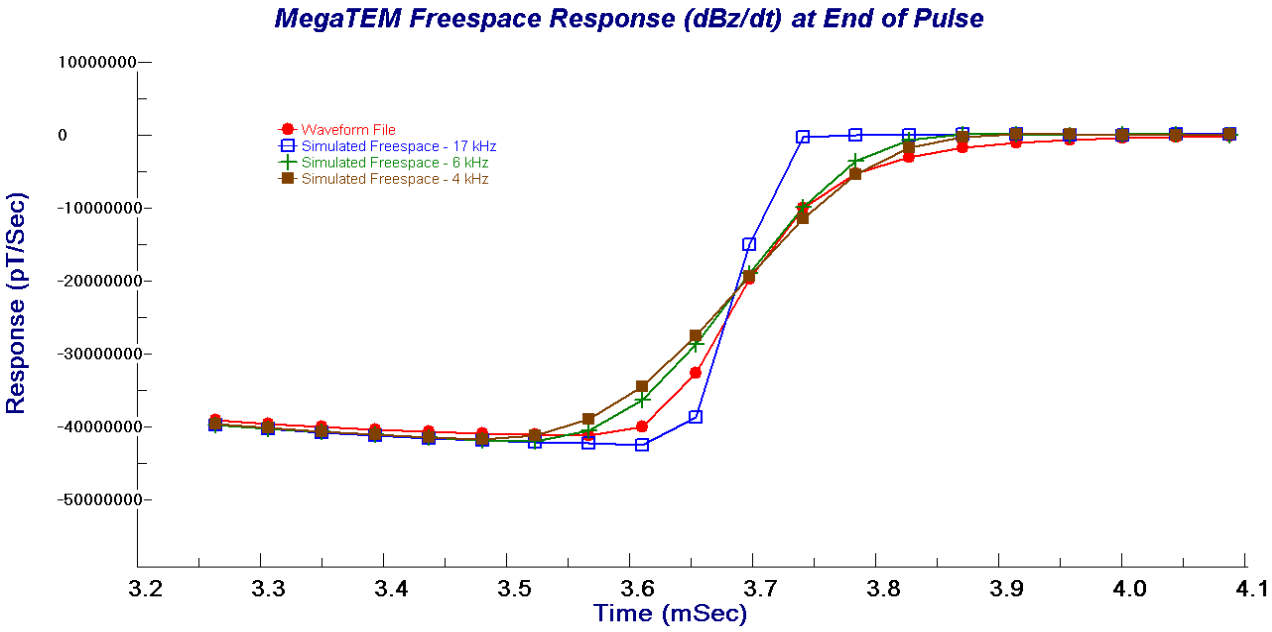

Figure 20: Comparison of dBz/dt at the end of the pulse for a MEGATEM waveform file (red) and the simulated freespace response for upper bandwidths of 17 kHz (blue), 6 kHz (green), and 4 kHz (brown).

4.4 Comparison with Ground Results

4.4.1 North-South Variation

South of 4200N, the response of Model 4S is too small at early times when compared to the data. As with the MEGATEM, the response of the model reaches a maximum misfit with the data at the south end of the calibration site. Shallow conductance is needed to increase the amplitude of the response. The most likely cause of this shallow conductance based on the geology of the site is a deeper layer of lower resistivity within the Moenkopi or at its base. Both the MEGATEM and the GEOTEM have insufficient shallow resolution to distinguish between a lower resistivity layer within the Moenkopi, and either an increase in the thickness of the top layer or additional conducting material near the surface. This increase in early time response to the south is observed not only on Line 12440 but nearby lines as well.

4.4.2 Comparison of North and South Ground Models

For the PROTEM survey, it was found that decreasing the thickness of the limestone in Model 4S by 13 m (this is Model 4N) improves the fit with the stations from 4400 north. However, for the MEGATEM data, Model 4S was a better fit than Model 4N north of 4400. Thus, the MEGATEM suggests a slightly greater depth to the Coconino north of the wash than the ground data. The responses of Model 4S and Model 4N for the GEOTEM were compared with the measured to data to see if this was observed for the GEOTEM as well. However, it was found the GEOTEM data cannot distinguish between models 4S and 4N as the data is too noisy from late mid-times (Figure 21).

4.4.3 Sensitivity of GEOTEM to Coconino/Hermit and Supai Group

It was found that the MEGATEM has some sensitivity to the Supai Group, but it cannot be used to accurately determine the depth to the Supai, unlike the wide-offset PROTEM data. The sensitivity of the GEOTEM was examined as well by removing the Supai Group from Model 4S by assuming the Hermit continued indefinitely. The results for the GEOTEM are the same as for the MEGATEM: removing the Supai Group from the model decreases the response at later channels. Unlike the difference between Model 4S and Model 4N, this is significant in comparison to the noise level of the data.

4.5 Noise

The GEOTEM data is much noisier than the MEGATEM. This is likely partially a result of the lower dipole moment, which is about half that of the MEGATEM but also could be associated with other aspects of the technology.

Clearly a high signal-to-noise ratio is desirable in the data. A geophysicist may wish to build an accurate model of the subsurface resistivity, but if the data is noisy it increases ambiguity in the model. For example, in section 4.42, it was shown that the difference between Model 4S and Model 4N is within the noise range of the GEOTEM. On the other hand, the difference between these two models is significant in comparison to the noise level in the MEGATEM.

In a more resistive environment, the high noise level in the GEOTEM may be even more problematic. If the subsurface resistivity were higher, the response would be smaller. Thus, if the same amplitude of noise was observed, the signal-to-noise ratio would be even lower than at the calibration site. If the signal-to-noise ratio were sufficiently small, the late time data would not be meaningful. In contrast, a system with a lower noise level may have useful data at the same times.

4.6 Summary

Similar to the MEGATEM, the GEOTEM generally agrees with the ground model at the north part of the calibration site if the bandwidth is adjusted to 6 kHz. It also suggests an increase in shallow conductance to the south, which, based on our geological understanding of the site, is likely a layer of low resistivity within the Moenkopi or at the bottom of the Moenkopi.

For both the MEGATEM and GEOTEM, rewindowing of the data to have 20 off-time channels was critical for understanding the response. The GEOTEM data, however, is noisier than the MEGATEM, likely as a result of having a lower dipole moment.

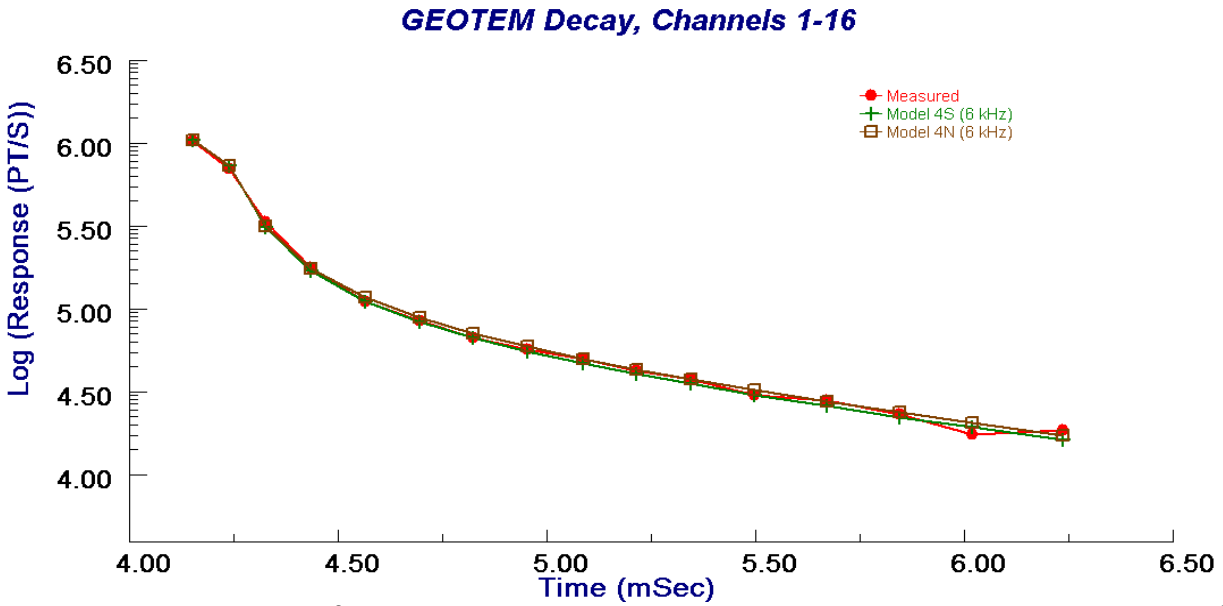

Figure 21: Comparison of measured MEGATEM Hz data (red) with the simulated response for Model 4S (green) and Model 4N (brown) on Line 12440 at (650E, 4872N) at early-mid times.

5.0 VTEM

5.1 Introduction

A large VTEM survey was flown in a region south of the Grand Canyon but data was also collected over the calibration site for calibration with other airborne systems and ground data. Two VTEM systems were used for the large survey: v7 and v11. At the calibration site, the data was collected only with the v7 system.

In the early VTEM data, current waveforms had a quarter sine turn-on followed by a constant current, and then a quarter sine turn-off that was equivalent to the turn-on. This was according to Geotech's specifications. The waveform in Geotech's report for this survey (Figure 22) appears to have these characteristics. It is described in the text of the report simply as a trapezoid waveform.

The first waveform delivered for this survey consisted of what were thought to be quarter sine turn-on and turn-off, but with steps in the current amplitude in between them. For the v11 system, there were additional steps in the turn-on. These steps in the current are pulses in the coil response, as seen in the waveform file for the initial flight over the calibration site (Figure 23). Current waveforms of the original forms were requested and Geotech thereafter provided what was originally considered to be of this form for both systems.

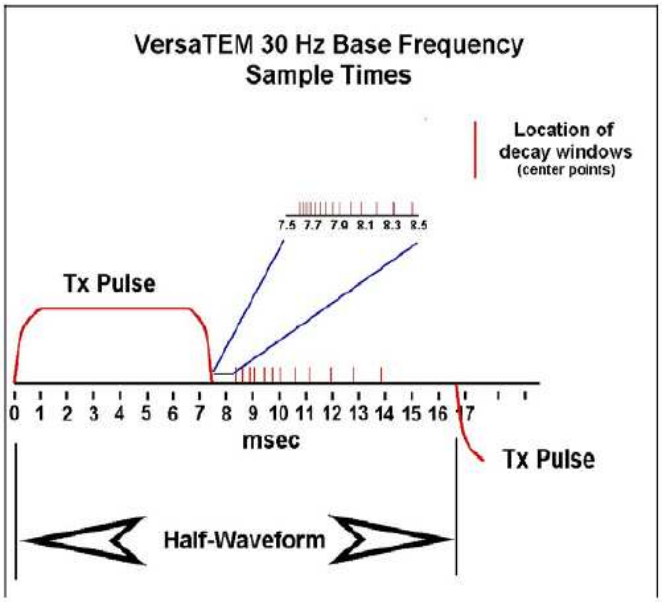

Figure 2 - VTEM Waveform & Sample Times

Figure 22: From Figure 2 of the report provided by Geotech for the VTEM survey.

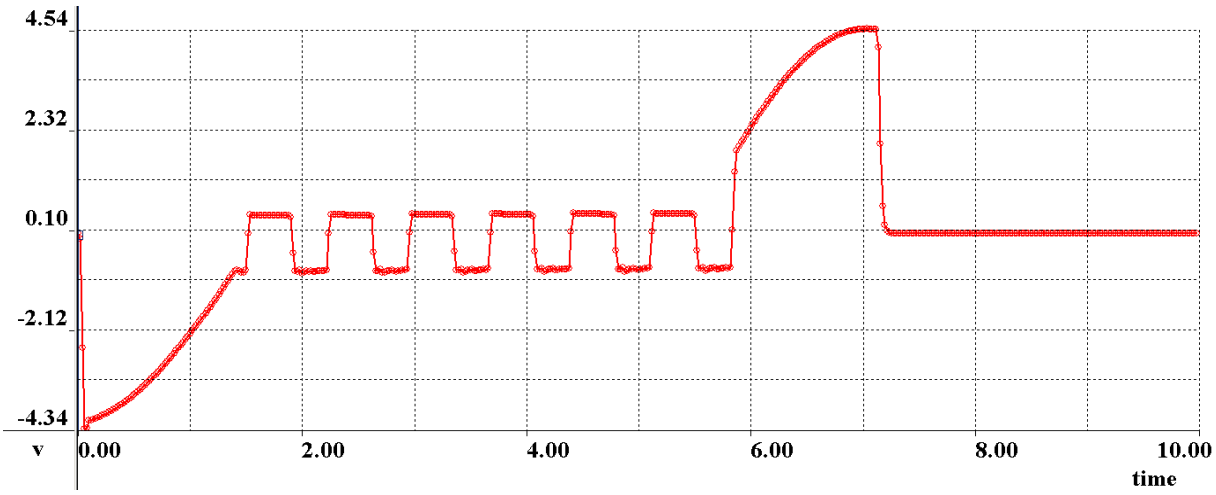

Figure 23: The first polarity of the preliminary v7 waveform provided by Geotech.

There were several concerns with the initial waveforms, which is why the second waveform type was requested. Each step in the current is a pulse in dB/dt and acts as a source. These may also interact, creating a more complex response and making it more difficult to visually interpret decays. As we were not interested in simply picking anomalies, but wanted to perform detailed accurate modeling and inversion, it was critical to be able to reproduce the waveform and visually interpret the decays in the background geology. As the steps in current amplitude seemed designed to produce a maximum current prior to turn-off it was felt that these step-ups in current may not be properly controlled through any given flight and thus the waveform would not be consistent across a flight or indeed the entire survey.

The data in the calibration area that is discussed in this report was collected with the second, probably more controlled waveform. Only Hz was measured. The data provided by Geotech is reduced by dipole moment and has units of $pV/m^4/A$. However, as discussed later, it is not clear at which point in the cycle the dipole moment is determined for normalization. This is more critical in that the multiple cycles are stacked to produce a measurement average at any given data point.

The VTEM has some potential advantages over the other systems for shallow resolution. Firstly, the decays are quite clean. Secondly, there are more channels: 28 versus 20 for the rewindowed MEGATEM and GEOTEM. The additional channels and clean decay should offer more discrimination in decays. 28 channels is nearly twice as many off-time channels as in the original MEGATEM data. Additionally, the VTEM system is closer to the ground with an average altitude of approximately 35 m for this system rather than 70 m for the MEGATEM receiver and thus likely to give more resolution in the shallow structure which was considered preferential for detecting the breccia pipes.

5.2 Initial Modeling

5.2.1 Initial Waveform

The initial simulation of the ground model (Model 4S) for the VTEM data was performed using a waveform with an equal quarter sine turn-on and turn-off as described in 5.1. A high bandwidth (170 kHz) was used as it was our understanding from the manufacturer that the receiver components had this rather high frequency content. The waveform settings for the initial simulation were based on analyses of the waveform file for the flight provided by Geotech. A pulse width of 4.46 ms and a frequency of turn-off of 162 Hz were used. This frequency of turn-off was determined by estimating the length of the turn-off (1.54 ms) and then assuming that the turn-off was full quarter sine. However, the response of Model 4S when these settings are used is a poor fit to the data on Line 700. The model response is too small at early times and too large at late times when compared to the actual VTEM data (Figure 24).

It should be recalled that for the MEGATEM and GEOTEM, the ground model (Model 4S) fit the airborne data north of 4200N when the bandwidth was adjusted. Unlike these airborne systems, however, adjustment of the bandwidth alone for the VTEM is insufficient for the ground model to fit the data, as bandwidth modification would not affect the simulation of the late time data. Furthermore, a simple adjustment to the upper bandwidth does not alter the early time response of the model such that it fits the shape of the decay in the measured data. Additionally, reasonable errors in the altitude of the system would not sufficiently affect the response. As a result, we considered that it was probable the misfit issue was related to the waveform. We began to investigate this waveform issue more deeply by closer analyses of the VTEM waveform file at the calibration site.

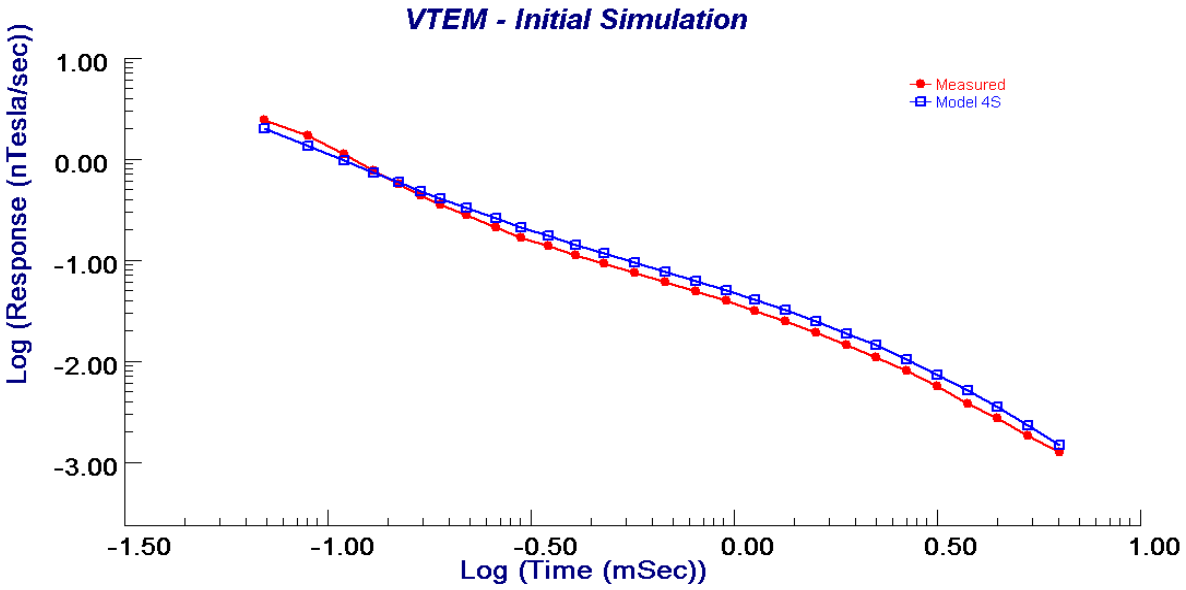

Figure 24: VTEM data (red) vs. response of Model 4S (blue) for the initial simulation (quarter sine turn-on and turn-off) at 4347 N on Line 700.

5.3 Waveform file

Initially, the waveform file was used to determine the pulse width and turn-off time as described in 5.2. Following the preliminary modeling results, a more detailed study of the waveform file was conducted to determine if it agreed with the waveform specified previously by Geotech, which is the waveform that was used for modeling. Both the original file (a time derivative waveform) and the integrated waveform (current form) were analyzed.

5.3.1 Original Waveform File

Geotech provided waveform files for each flight in the survey. The waveform file for the calibration site flight was studied, along with several other waveform files for the survey. Each of these file contains two full cycles. The sampling is 50 kHz and the response is recorded in volts. This is thought to be the dBz/dt coil response, and its shape corresponds to the derivative of the current waveform. However, it is not actually known how the waveform data were collected. In contrast, for GEOTEM and MEGATEM, it is known that the waveform data are collected at high altitude, and the response of the transmitter and each of the coils (both dB/dt and B) are given. The information contained in the VTEM waveform files is more limited. Additionally, the Fugro systems indicate time windows from the origin of the cycle whereas VTEM is indicated from the end of turn-off. However, the determined turn-off relative to the beginning of the cycle is not given for the VTEM data. This appears to be a critical issue.

5.3.1.1 VTEM Waveform Features of Interest

Figure 25 shows both polarities in the first cycle of the waveform file for the calibration site. The second cycle is very similar, though not identical.

The waveform is considered to be comprised of three sections: the turn-on, ramp-up and turn-off, as marked in Figure 25. There are several features of note in the waveform. While we had expected the current to be constant between the end of turn-on and beginning of turn-off, it is clear that the current is ramped up, as the coil response is not zero during this time. Furthermore, the coil response is not constant, but decreases slightly in amplitude when approaching the turn-off. Therefore, the increase in current is not perfectly linear. It is also observed that the turn-on and turn-off have somewhat different shapes, whereas they were expected to be equivalent. Additionally, the two polarities differ slightly from each other: the first polarity has a lower response in the turn-on, but a greater response in the turn-off.

Several interesting features were also observed that relate to the upper bandwidth of the system (see Figure 25). Firstly, the sharp spike at the beginning of the turn-on, which is particularly evident in the first polarity, suggests very high frequency content in the system. However, at the beginning of the ramp-up, the ringing in the waveform suggests a much lower bandwidth. After turn-off, there is no ringing in the waveform so it is thought that a heavy low-pass filter must have been applied digitally at this stage. Thus different parts of the waveform seem to indicate different bandwidths for the system. We have no knowledge of the reasons or sources of these differences.

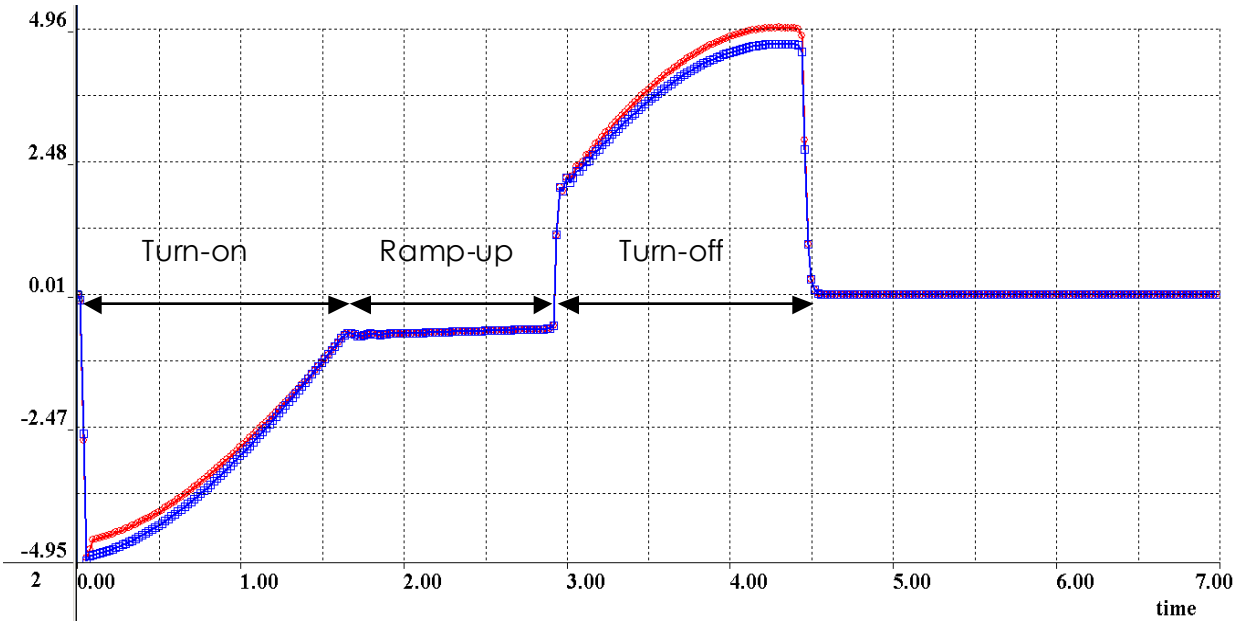

Figure 25: VTEM waveform provided by Geotech for test site – comparison of first polarity (red) and second polarity with the sign flipped (blue).

5.3.1.2 Comparison with Other Waveform Files

The waveform at the calibration site has similar characteristics to the waveforms for other flights in the same project for both v7 and v11 systems. The lengths of the pulse, turn-on, and turn-off are fairly consistent in other flights, with the pulse width varying by no more than 0.01 ms. All waveform files examined also have spikes in the response at the beginning of the turn-on and ringing following turn-on.

There are, however, slight differences in the amplitude in the waveform files, particularly at the beginning of the turn-on and the end of the turn-off. For example, in a study of fifteen v7 waveform files over five days (May 14-16, May 26, and June 13), it was found that the amplitude before turn-off ranged from 4.876 to 5.041 V for the first polarity. Conversely, at the beginning of the ramp-up and the beginning of the turn-off, the values are very similar in the different Uranium One waveform files. It is interesting that the ringing at the beginning of the ramp-up and the beginning of the turn-off is quite consistent in the different waveform files. At a point just after turn-off begins, values range from 1.992 to 2.004V. A comparison of the turn-off for first polarity for the three of the fifteen waveform files examined is shown in Figure 26.

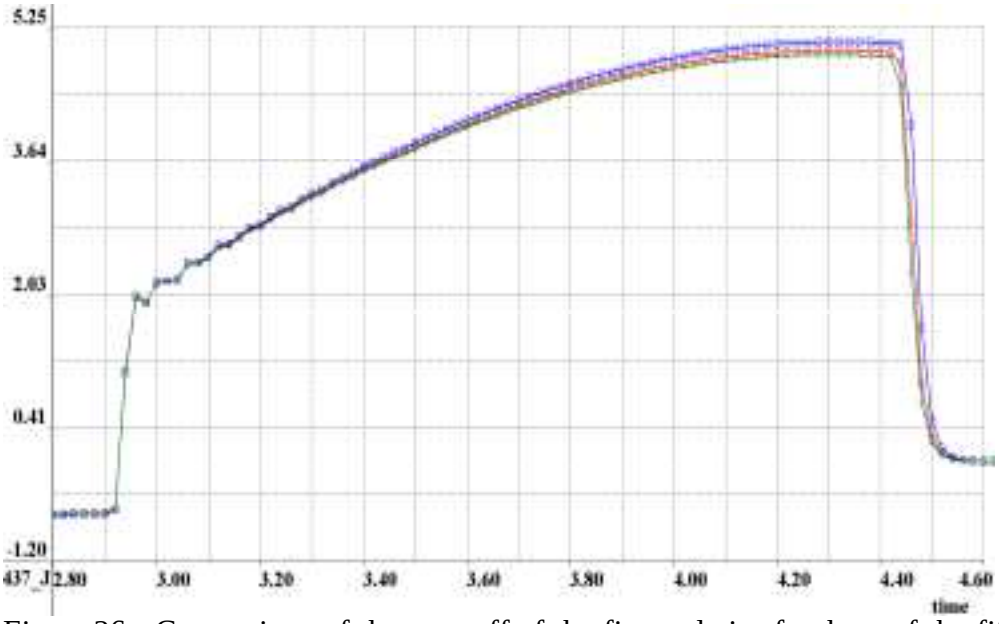

Figure 26: Comparison of the turn-off of the first polarity for three of the fifteen v7 waveforms that were studied. Red is the calibration site flight, blue is the flight with the largest amplitude (Flight 372) and green is the flight with the smallest amplitude (Flight 437).

In the waveform file for the calibration site, it was observed that the difference between the two polarities was about 6.5%. This is consistent with the other v7 waveform files examined, in which the difference is 6.1% - 7.0%. For other bipolar waveform systems, the data from the two polarities are differenced and then averaged. How this discrepancy between polarities of the VTEM system is handled is not known. If the two polarities are appropriately weighted when averaging polarities then this would not be a source of error. However, if the first or second is utilized for the stack weighting then this would be a source of a 3% error in the response amplitude.

The waveform files for the v11 system have the same characteristics as the v7 waveform files. However, the amplitude at the beginning of the ramp-up and beginning of the turn-off are slightly different from the v7 files. As noted, these values were quite consistent across v7 files and are similarly consistent across v11 files, but there are minor differences between the v7 and v11 values. Interestingly, the difference between the two polarities is not observed in the v11 waveform files prior to May 17 after a number of days of flying, though on later v11 flights, the difference in the two polarities is similar to that observed for v7.

The VTEM waveform files for the Uranium One survey were also compared to waveform files from other projects with a 30 Hz base frequency. Files are available from 2006-2008. It was found that there are two general types of waveforms. The first has a short pulse, similar to the 4.46 ms pulse observed in the calibration site waveform file. The second has a long pulse, about 7.1 ms, and several short pulses in the coil response, which correspond to steps in the current waveform. This was the preliminary waveform described in 5.1.

The waveforms for this survey are very similar to other waveforms with the short pulse. The lengths of the pulse, turn-on, and turn-off are fairly similar in all of the files examined. The shape of the turn-on and turn-off, and the ramp in between the turn-on and turn-off are very similar in nature as well. The spike in the waveform at the beginning of the turn-on and the ringing after the completion of turn-on are also observed in other waveform files. The only significant difference is that in two of these waveform files, both polarities are nearly identical.

The preliminary waveform for this survey is quite similar to other waveforms with a long pulse. They all contain several small pulses in the ramp-up, and most also contain these pulses during the turn-on as well (like the preliminary v11 waveform). The shape of the turn-off is similar in all cases.

5.3.2 Integration of waveform

The waveform was integrated in an attempt to obtain the shape of the actual current function and the result for the first polarity is shown in Figure 27. This purpose of the integration was to obtain a clearer picture of the waveform and to better characterize the nature of the turn-off.

In the integrated waveform, the increase in current between the turn-on and turn-off is clearly seen. The response immediately before turn-off (the peak in the waveform) is about 18% greater than the response immediately after turn-on.

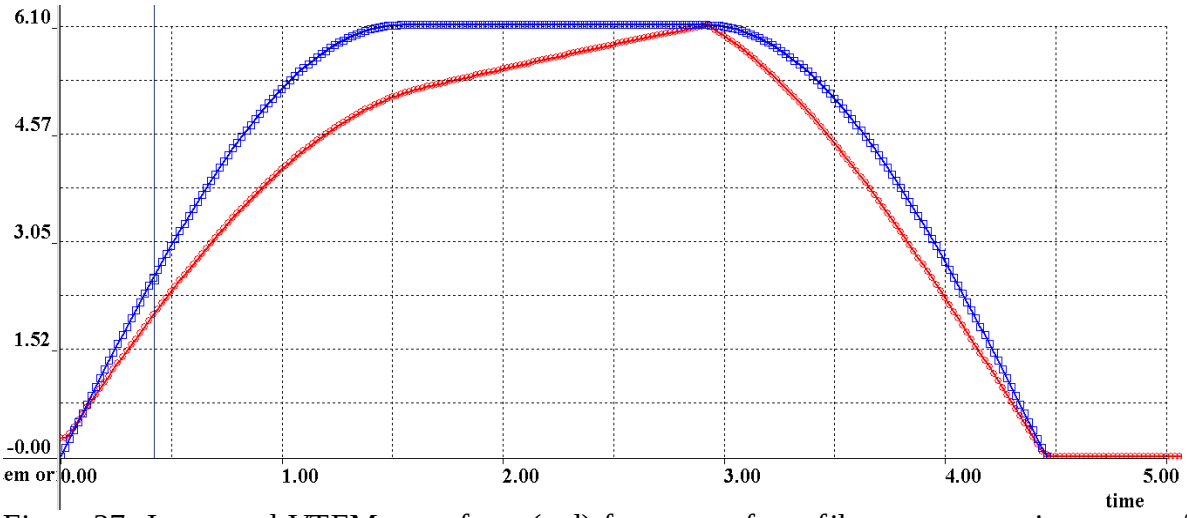

Figure 27: Integrated VTEM waveform (red) from waveform file vs. quarter sine turn-on/turn-off waveform (blue) used for initial simulation.

A closer examination of the turn-off revealed that it is not well-modeled by a quarter sine (162 Hz) turn-off; in fact, it falls between a linear ramp-off and a quarter sine turn-off (Figure 28). It was found that this could be approximated by a 125 Hz sine function with the same 1.54 ms length of turn-off (ie, 77% of a quarter of a 125 Hz sine function). Thus, the nature of the turn-off is significantly different from our initial understanding of the waveform.

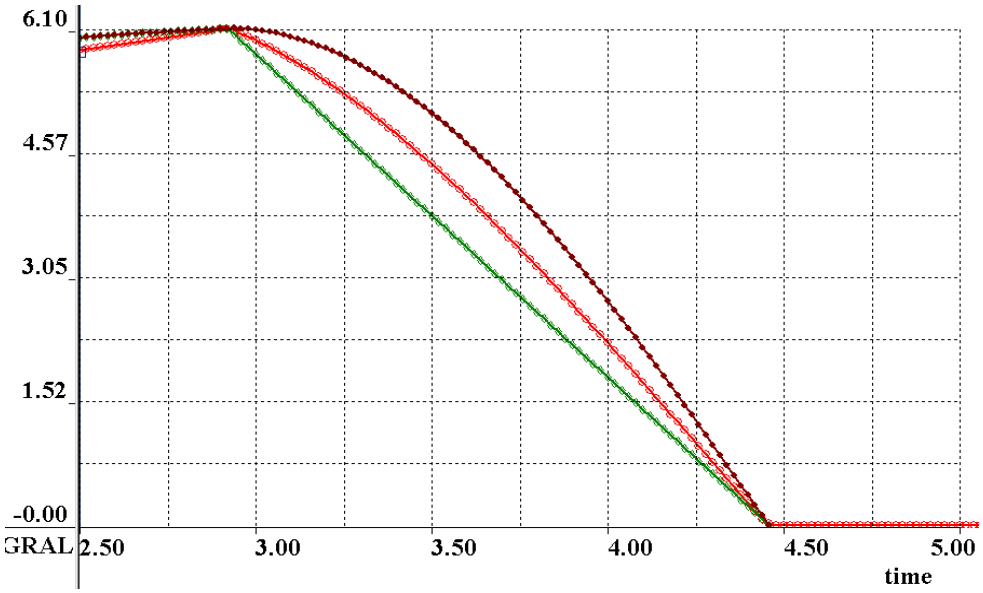

Figure 28: Turn-off of the integrated VTEM waveform (red) vs. a ramp turn-off (green) and a quarter sine turn-off (brown).

The turn-on is also not a full quarter sine. It is slightly different in shape from the turn-of though, and is well-modeled by 87% of a 140 Hz quarter sine. Together, the turn-on and linear ramp-up in current can be approximated by an exponential function as follows with a decay constant of about 0.8 ms:

$$f(t) = A\,(1-e^{-t/\tau}) \qquad (1)$$

where A is the peak current, t is the time, and τ is the decay constant. This was chosen because it is the standard turn-on for ground systems and is a reasonable approximation for the turn-on of the integrated waveform.

Combining the exponential function and 77% of a 125 Hz quarter sine turn-off results in the waveform shown in Figure 29, which matches the integrated waveform much more closely than the waveform initially used for modeling in Figure 27.

Integration of the preliminary waveform, which had multiple pulses, was also performed (Figure 30). It was found that the turn-off of this waveform was also about 77% of a quarter sine, but since the turn-off time was shorter (1.28 ms vs. 1.54 ms), the frequency of turn-off was higher (150 Hz vs. 125 Hz). Thus, the nature of the turn-off is consistent in both the short-pulse and long-pulse waveforms.

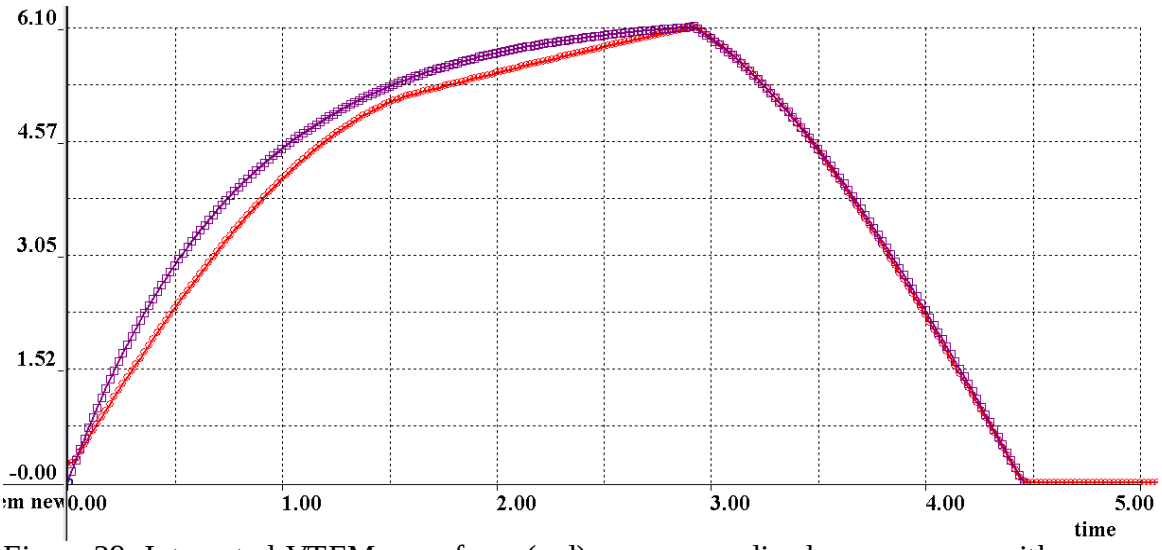

Figure 29: Integrated VTEM waveform (red) vs. a generalized square wave with an exponential turn-on and a 125 Hz sine turn-off with a turn-off time of 1.54 ms (purple). This is the new waveform used for simulation and is a good approximation of the waveform provided by Geotech.

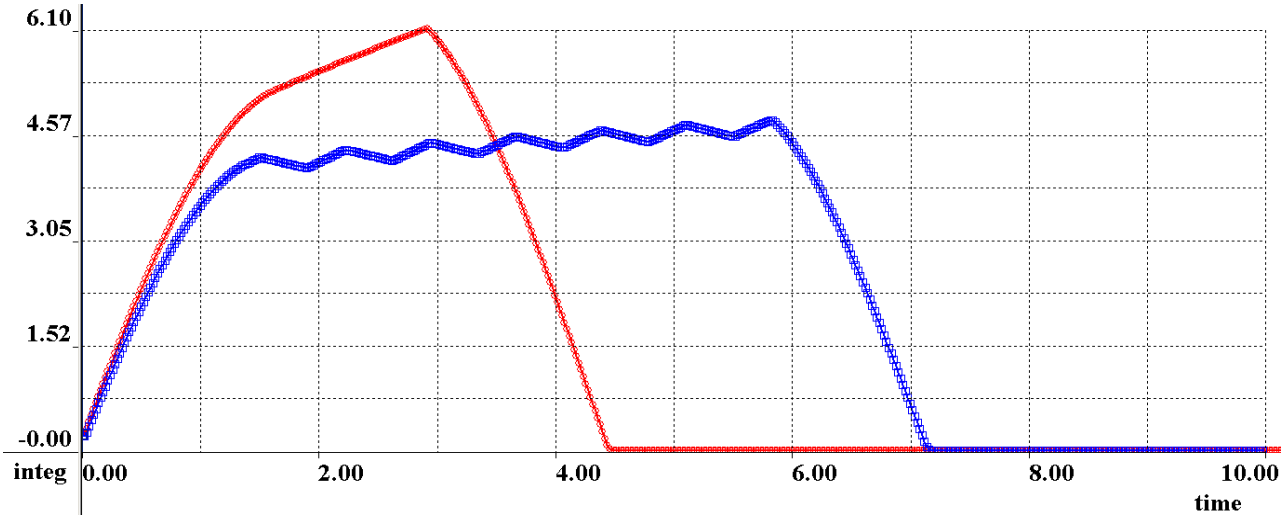

Figure 30: Comparison of the integrated waveform at the calibration site (red) seen in Figure 26 to the integrated preliminary waveform (blue).

The results of integrating the waveform files show that the actual VTEM waveform differs from what we had understood from Geotech. We considered that the VTEM waveform may have had a quarter sine turn-off some years ago, but that the turn-off has since been adjusted. To test this hypothesis, we analyzed waveform data from 2003. Upon integration of the waveform, it was found that while the turn-off was not quite a quarter sine, it was about 89% of a quarter sine. In contrast, recent waveforms have a turn-off that is about 77% of a quarter sine. Additionally, the length of turn-off was shorter at 0.92 ms. It appears that there has been some change in the nature of the turn-off in the VTEM system.

5.4 Further Modeling

These analyses of the waveform file revealed that it was different from what had initially been used for modeling. In this section, we examine whether Model 4S would fit the VTEM data if we more closely match the current waveform in the waveform file, as determined from integration in 5.3.2.

We chose to use our modified waveform shown in Figure 29 rather than the actual integrated waveform as this would allow us to better study which aspects of the waveform were most important to the response, as we could easily change one or more settings.

5.4.1 Modeling of VTEM Response

We consider the output response of the system to be a convolution of the current impulse response with the current input function and the system response of the both transmitter and receiver. In frequency domain,

$$H(\omega) = I(\omega)T(\omega)S(\omega)R(\omega) \qquad (2)$$

where $H(\omega)$ is the output, $I(\omega)$ is the current function, $T(\omega)$ is the system response of the transmitter, $S(\omega)$ is the response of the earth and $R(\omega)$ is the system response of the receiver. Thus, we ensure that the waveform convolution is ensured to be precise by building it independently by controlling its basic properties.

We are able to model several different types of current waveforms. The specifications of the waveform, such as the pulse width, can be adjusted. When making the changes to the VTEM waveform described below, the waveform was checked with the modeling by simulating the freespace B-field during the pulse.

5.4.2 Turn-on Issues

Initially, we changed only the turn-on of the waveform, using equation (1) with τ=0.8ms as described above to model the turn-on and subsequent ramp-up of the current. The turn-off was still represented by a full quarter sine turn-off. The response using this waveform differed only slightly at late times from the response of the initial representation of the VTEM waveform. This indicates that the system is not very sensitive to the nature of the turn-on. We also experimented with different values of τ and found it had little effect on the response.

Although the system is not very sensitive to the nature of the turn-on, it is sensitive to when the turn-on begins. It was found that significantly increasing the pulse width, which moves the beginning of turn-on earlier in time, has a very small effect on the early time but increases the late time response. While an adjustment to the pulse width was not required to better approximate the integrated waveform in Figure 29, these results are applicable to the longer VTEM pulse. This longer, 7.1 ms pulse would be expected to result in a greater late time response than the shorter 4.46 ms pulse.

5.4.3 Turn-off

In the second adjustment to the waveform, we changed the turn-off from a quarter sine to a 125 Hz turn-off frequency with the same length of turn-off, as had been determined from the waveform file. When Model 4S was simulated with this waveform, the response of the model

was 15% greater than the data at mid-late times, but too small at early times (Figure 31). The response is lower than the simulation with the initial waveform across all channels.

With some additional modeling, it was concluded that the rate of turn-off at the end of the on-time has a particularly large effect on the response in the off-time. A higher rate of turn-off (i.e., a greater amplitude of dB/dt) results in a greater response across all time channels, though the effect was slightly larger at early times than at late times. For example, in Figure 28, it is clearly observed that a quarter sine turn-off has a much greater rate of turn-off at the end of the pulse than a ramp, where both have the same length of turn-off. The quarter sine turn-off has a much larger response as noted above.

Further illustrating the importance of the rate of turn-off at the end of the pulse, it was found that half-sine and generalized square wave (turn-on as in equation (1) and linear ramp off) with a 1.39 ms ramp turn-off have very similar responses. Despite the significant differences between the two waveforms, the early time response was nearly identical, and the mid-late time response had slight differences only. This is caused by the nearly identical rates of turn-off at the end of the pulse for these two waveforms.

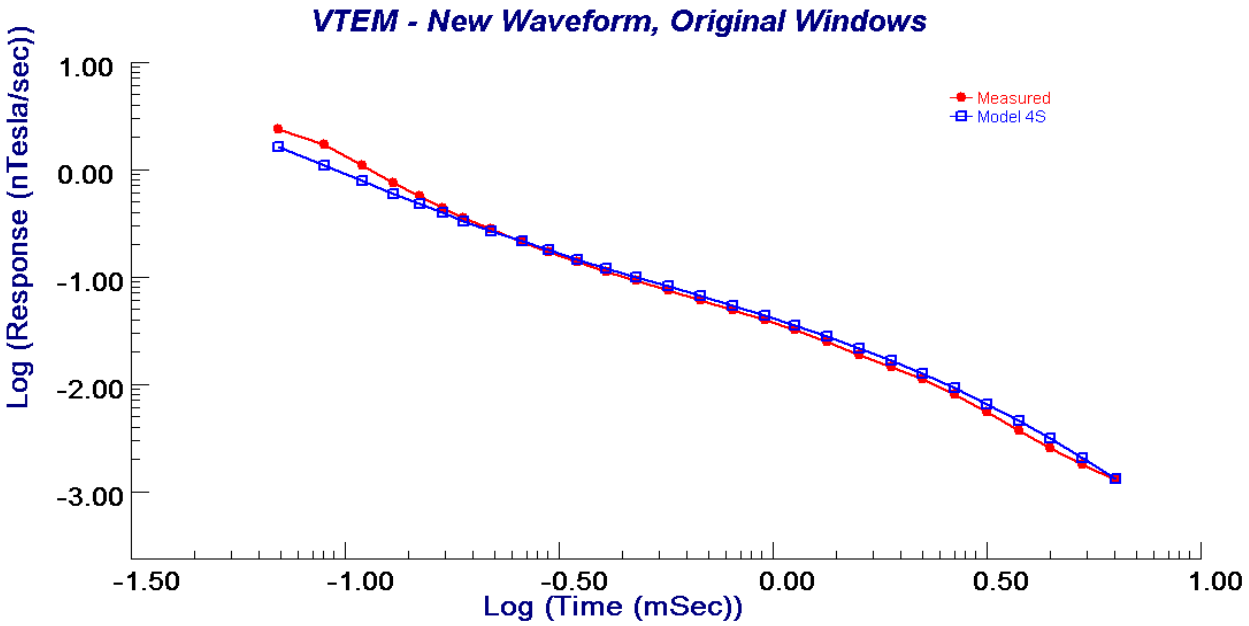

Figure 31: Measured VTEM (red) at 4374N vs. Model 4S (blue), simulated with the modified waveform.

5.4.4 Early Time Misfit

The misfit at early times could be due to an issue with the time channel positions. In fact, shifting the time windows earlier by 0.03 ms increases the early-time response such that it results in an amplitude factor of 1.15 between the simulated VTEM response to Model 4S and the VTEM data (Figure 32) with the exception of the first channel. This shift has little effect on the simulated response at late times but it has a considerable effect on the response at early time

channels. A shift of 0.03 ms is very significant in the early time channels, which are fairly close to the end of the pulse. The first time channel was originally centered at 0.07 ms, and the first seven channels are all 0.02 ms apart. Thus, this shift in the time windows is essentially shifting them earlier by 1.5 time windows.

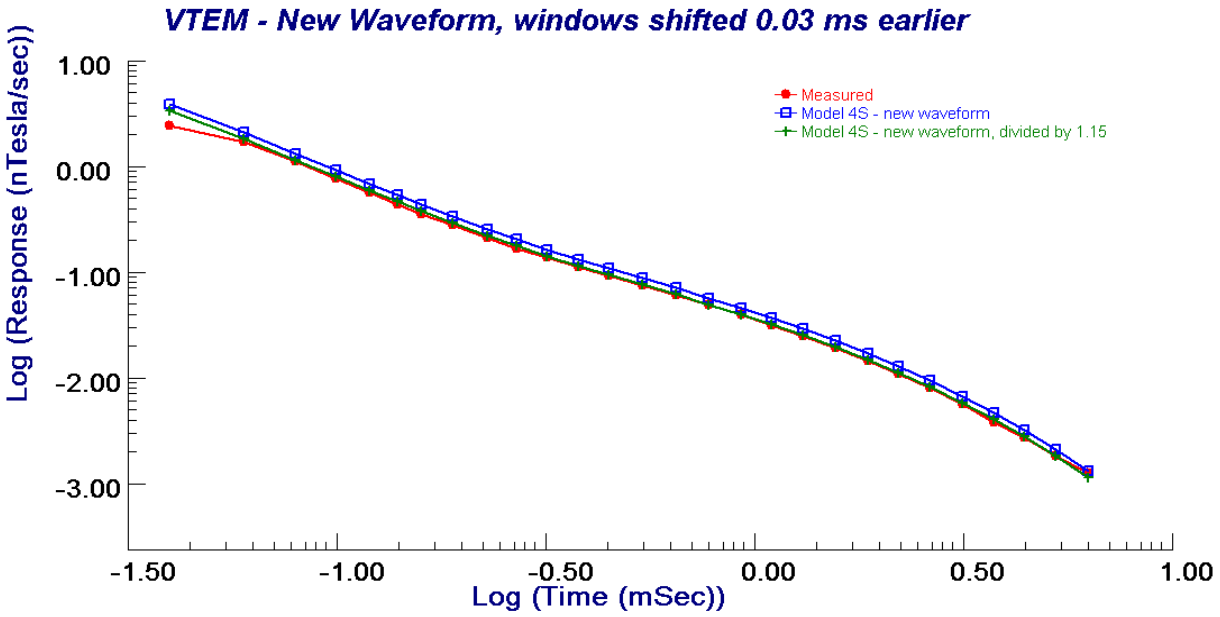

Figure 32: VTEM data (red) vs. response of Model 4S (blue) for the new VTEM waveform at 4347N with the windows shifted 0.03 ms earlier in time. Its amplitude is approximately 15% to high. In green is the response of Model 4S divided by 1.15.

The issue with the time channels positions may be due to Geotech's definition of time zero. It was assumed that the time channels were in reference to the end of the pulse. However, because the system is band limited, the coil response begins to decrease before the end of the pulse. Based on the waveform files, the response starts to diminish about 0.02-0.03 ms before the end of the pulse (Figure 33). If the time channels are actually in reference to when the coil response begins to decrease, then they would need to be shifted 0.02-0.03 ms earlier from the times given if modeling is performed using the end of the pulse as the reference. This shift of 0.02-0.03 ms is approximately the time shift needed for there to be a consistent amplitude shift between the model and data for channels 2-28, as noted above. Thus, this issue of how time zero is defined for the time gates is considered a likely cause of the early-time misfit. We do not have documentation that indicates the position of time zero.

The lack of information on the relationship between the timing of the pulse and the time channels for the VTEM is in contrast to the information that Fugro provides for their data. In the Fugro data, the channel times are given with respect to the beginning of the pulse plus a given delay time (100 µs). The pulse width is also given. Therefore, it is clear exactly where the channels are with respect to the pulse.

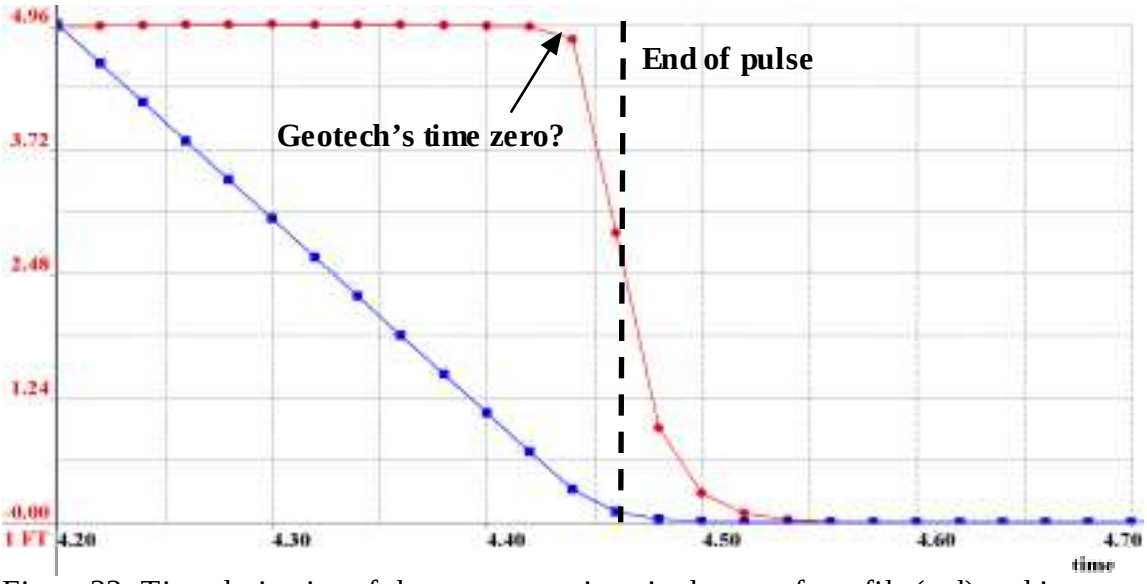

Figure 33: Time derivative of the current as given in the waveform file (red) and integrated waveform (blue) at the end of the pulse. Sample points are 0.02 ms apart.

5.4.5 Discussion of Amplitude Factor

Several possibilities were considered for the discrepancy of in amplitude of 15% observed between the model response and data after the time channels were shifted. The discrepancy in amplitude may be due to how the data is reduced by dipole moment, or this may be one of the contributing factors. VTEM data is always reduced by dipole moment, however, there are several uncertainties regarding how the dipole moment is determined, and also how the reduction is performed.

To determine the dipole moment, the transmitter loop area, number of windings in the transmitter loop, and the interaction between these windings are required in addition to the current. An error in any of these items would lead to an incorrect data amplitude after reduction by dipole moment. In this case the data is smaller than the model response, which could be the result of overestimating the dipole moment.

The first of these potential issues is this area of the loop. We would like to clarify the exact loop area that Geotech used when determining the dipole moment. Furthermore, based on the system specifications given, there are some uncertainties that must be resolved for us to calculate the area of the loop ourselves. Firstly, the diameter of the loop is given as 26 m in the final report and 26.2 m in the readme file accompanying the data. These two diameters correspond to a difference in area of about 1.5%. Furthermore, it is our understanding that the transmitter is a dodecagon, and as such, it is not clear to what the diameter refers. For example, the diameter given could be the distance from corner to corner, or from the center of one edge to the center of the opposite edge. The difference in area for these two possibilities is 7%, which is not insignificant.

In the final report from Geotech, it is stated that the transmitter has four windings. However, it is not clear whether the interaction between the multiple windings has been calibrated. An

interaction between them would decrease the dipole moment. Therefore, if this interaction is not considered, the data may be reduced by a dipole moment that is too large, resulting in the data being too small, as is observed at the calibration site. Similarly, there may be an interaction between the multiple turns of the receiver coil, and it is not known whether this has been considered.

Further relating to these dipole moment issues is the discrepancy between the dipole moment given in the final report, and that which we calculated by multiplying the number of turns, current, and area of the loop together. If the loop area is calculated using the formula for the area of a circle (assuming a diameter of 26 m), then the dipole moment calculated is 424,740, whereas the dipole moment given in the report is 395,000, about 7% less. Even if the area is calculated for a dodecagon (assuming the diameter is either corner-to-corner or edge center to edge center), the calculated dipole moment is still more than that given in the report. It is not clear if the lower dipole moment given in the report is to account for the multiple windings of the transmitter, or if this is in error. It was noted that in the report for a different VTEM survey, in which the current, number of turns, and loop diameter were the same as in the calibration site survey, that the given dipole moment matched our calculations

The issue is not simply how the dipole moment is determined, but also how the reduction is performed. For example, we are not certain where in the cycle the current is determined for normalization. It was assumed that the peak current was used. Furthermore, it is unclear whether the reduction was performed based on monitoring of the peak current or monitoring of dB/dt. As well, it would be helpful to know whether the reduction is performed every cycle or every half-cycle. Due to the 6% difference in the two polarities, reducing by dipole moment only every cycle may result in a 3% error.

In addition to how the data is reduced by dipole moment, it is also possible that part of the amplitude shift observed is due to the tilt of the bird. It is our understanding that a tilt of 5-10% would be reasonable and that the receiver and transmitter would have the same orientation. Such a tilt would result in a reduction of the response of up to 2%. However, should the tilt be significantly more, the effect would be more pronounced.

5.4.6 Modeling of the VTEM Data

Modification of Model 4S to fit the VTEM data with the original time windows required significant changes to the resistivities. The resistivity of the Moenkopi must be dropped considerably to around 70 Ωm to increase the very early time response, and the resistivity of the limestone sequence must be increased to about 1700 Ωm (from 328 Ωm) to match the shape of the decay (Figure 34). Thus, even with an appropriate waveform based on the waveform file, if modifications are not made to the location of time channels and amplitude of the data, the resulting model will not be consistent with other information on the site.

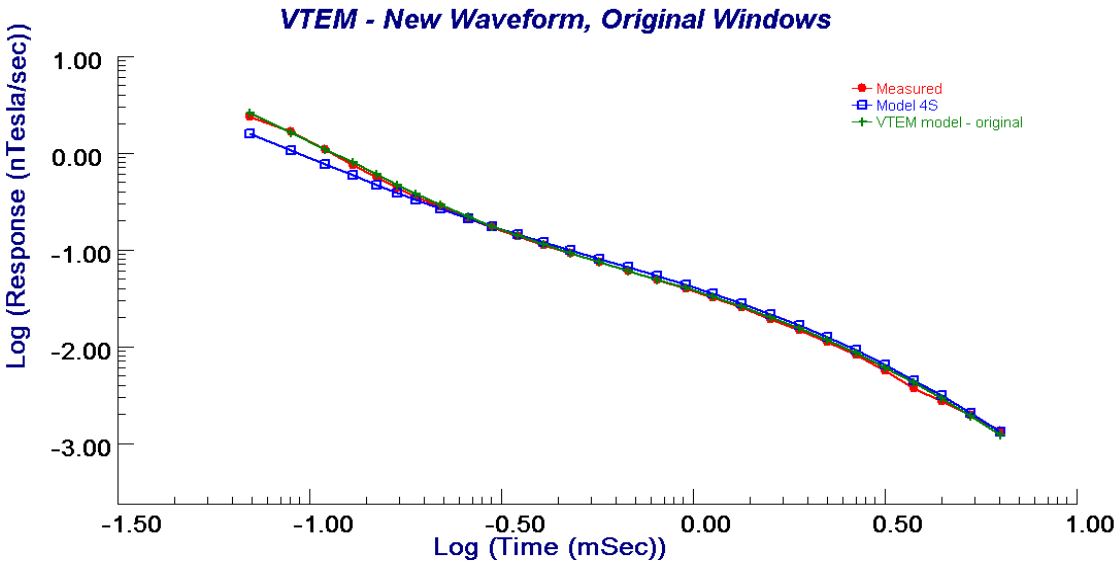

Figure 34: Comparison of the VTEM data at 4374N on Line 700 (red) with the response for Model 4S using the original time channels and new waveform (blue), and the response of a model that fits the VTEM data with these settings (green).

5.5 Additional Datasets

The results for the calibration site suggest an issue with the positioning of the early channels, and also an amplitude factor between the model and data. These results are supported by modeling of other datasets, including the preliminary VTEM data collected at the calibration site, and a study of an additional site.

5.5.1 Preliminary Data at Calibration Site

Model 4S was also simulated for the initial data which was collected with the preliminary waveform (shown in Figure 23). The same waveform shape was used as described in 5.3.2 as the nature of the turn-off was determined to be the same as that for the shorter pulse. The following parameters were used based on analysis of the waveform file: turn-off time of 1.38 ms, turn off frequency of 150 Hz, and pulse width of 7.1 ms. Note that this waveform does not capture the effect of the steps in the current turn-on though this is thought to be small.

The results are similar to the results for the 4.46 ms pulse: the response is too small at early times and too small at late times (Figure 35) In fact, the misfit is similar at late times to that observed with the 4.46 ms pulse. Therefore, the misfit between the data and model is consistent for two different waveforms.

5.5.2 Second Site

South of the calibration site there are several lines of VTEM that partially overlap with MEGATEM lines. This enabled us to determine whether there is a 15% amplitude shift between the VTEM and other systems at a different site. There is not, however, any ground TEM data in this area.

Here, we describe a site about 70 km E and 110 km S of the calibration site. The VTEM data was collected with the v11 system rather than the v7 system. The 0.03 ms shift was applied to the VTEM time channels before modeling. The ground is more resistive and the response is nearly an order of magnitude lower than at the calibration site. A 4-layer model fits the MEGATEM data reasonably well. The simulated data for this model is 15% too large for the VTEM data, the same factor observed at the calibration site once the channels were shifted earlier. A model that fits the VTEM must be more resistive, and has too low of an amplitude for the MEGATEM (Figure 36). Although the MEGATEM data is somewhat noisy, the simulation of the model that fits the VTEM data is outside the level of noise seen in the data. These results agree with our findings at the calibration site and indicate that the v7 and v11 data are consistent.

5.6 VTEM Summary

The results of the extended study of the VTEM waveform files and modeling show that if using the waveform provided by Geotech, the ground model does not fit the data. The response of the model is too small at early times. To get a consistent misfit across the decay, the time gates must be shifted 0.03 ms closer to the pulse. We suspect that this is due to how Geotech defines their time origin when providing the timing of the channels. After shifting the position of the channels 0.03msec early, the model response decays now have exactly the same shape as the data decays but the model is 15% larger than the data at channels 2-28. This we suppose is related to how the data is stacked and reduced by dipole moment. To properly model VTEM data, it is critical that we know how the data is reduced by dipole moment so that the amplitude of the response can be modeled correctly. Without adjusting the time windows and the amplitude of the VTEM response, the resulting model is significantly different in resistivity from the ground model. While we believe that the VTEM has better shallow resolution than the MEGATEM and GEOTEM, we conclude that more information on the system is required for accurate modeling.

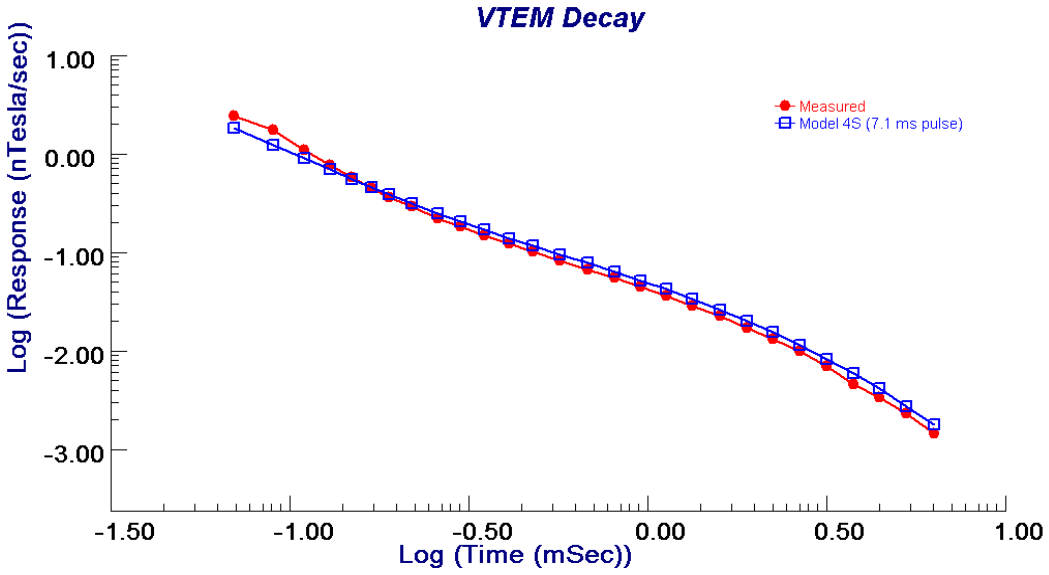

Figure 35: Comparison of VTEM data collected with preliminary waveform at 4376N and response of Model 4S.

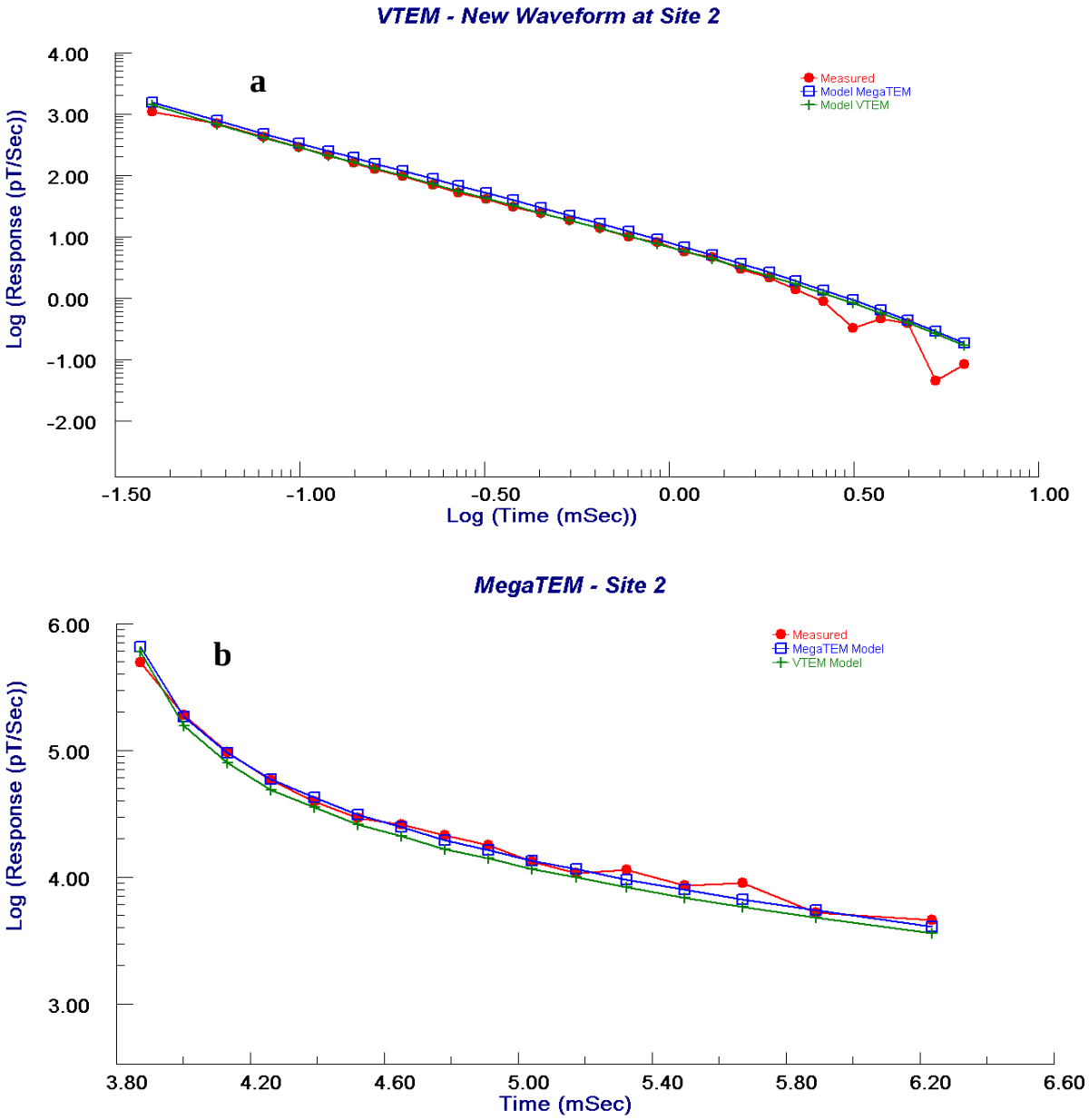

Figure 36: Comparison of the VTEM and MEGATEM data and models at site 2 at about 423540 E. A decay on line 2546 of the VTEM is shown in a) and a section of a decay on Line 2280 of the MEGATEM is shown in b). For the VTEM data, the channels have been shifted 0.03 ms earlier in time. Measured data is in red, MEGATEM model is in blue, and VTEM model is in green. The MEGATEM model's response is about 25% larger than the VTEM model response.

6.0 Overall Conclusions

The availability of data from three airborne TEM surveys at a test area near the Grand Canyon provided a unique opportunity for a comparison between these systems and TEM ground methods. It was determined that MEGATEM and GEOTEM data calibrate with the ground data. However, rewindowing was essential for understanding the response. VTEM data may calibrate with the other data, but more information on system settings is needed.

The results for this case study show the usefulness of fixed-loop ground TEM for mapping sedimentary environments. Using a PROTEM fixed loop survey that included stations at large offset, a layered resistivity model that matches geological information was developed. We were able to detect a layer about 500 m in depth, and also detect a small north-south change in structure.

Our findings also highlight the importance of accurately knowing system parameters for effective interpretation of airborne TEM. These include pulse width, exact window locations, waveform details, and impulse response of the receiver coils. All of these aspects must be accurately represented in modeling and inversion algorithms. Specifics for the MEGATEM and GEOTEM surveys were readily available from information provided by Fugro and using the correct system settings, the ground model matched these data reasonable well once the bandwidths were determined. However, information available for the VTEM was more limited. When the ground model was simulated for VTEM to our best knowledge of system settings, including closely matching the current waveform as determined from integration of the waveform file, the model response did not match the data. This discrepancy may be because we are not modeling critical aspects of the system of which are not aware. Knowledge of how the data is reduced by dipole moment and how the positions of the time windows are defined with respect to the pulse would assist us in modeling the VTEM response.

Acknowledgements

The authors would like to thank Uranium One for the use of their data and to acknowledge the contributions to this paper from Petra Webb and Ron Haycock of Uranium One USA.

References

Groom, R. and R. Jia, 2005, On time-domain transient electromagnetic soundings: 18th Annual Meeting, SAGEEP Proceedings, 514.

Jia, R., and R. Groom, 2007, Enhancing Model Reliability from TEM Data Utilizing Various Multiple Data Strategies: 20th Annual Meeting, SAGEEP Proceedings.